

Holographic entanglement entropy probe on spontaneous symmetry breaking with vector order

Chanyong Park,^a Gitae Kim,^b Ji-seong Chae^b and Jae-Hyuk Oh^{b,*}

^a*Department of Physics and Photon Science, Gwangju Institute of Science and Technology, Gwangju 61005, Korea*

^b*Department of Physics, Hanyang University, 222, Wangsimni-ro, Seongdong-gu, Seoul 04763, Korea*

E-mail: cyong21@gist.ac.kr, kingitae728@gmail.com, mp3dp98@hanyang.ac.kr, jaehyukoh@hanyang.ac.kr

ABSTRACT: We study holographic entanglement entropy in 5-dimensional charged black brane geometry obtained from Einstein-SU(2)Yang-Mills theory defined in asymptotically AdS space. This gravity system undergoes second order phase transition near its critical point, where a spatial component of the Yang-Mills fields appears, which is normalizable mode of the solution. This is known as phase transition between isotropic and anisotropic phases, where in anisotropic phase, SO(3)-isometry(spatial rotation) in bulk geometry is broken down to SO(2) by emergence of the spatial component of Yang-Mills fields, which corresponds to a vector order in dual field theory. We get analytic solutions of holographic entanglement entropies by utilizing the solution of bulk spacetime geometry given in [arXiv:1109.4592](https://arxiv.org/abs/1109.4592), where we consider subsystems defined on AdS boundary of which shapes are wide and thin slabs and a cylinder. It turns out that the entanglement entropies near the critical point shows scaling behavior such that for both of the slabs and cylinder, $\Delta_\epsilon S \sim \left(1 - \frac{T}{T_c}\right)^\beta$ and the critical exponent $\beta = 1$, where $\Delta_\epsilon S \equiv S^{\text{iso}} - S^{\text{aniso}}$, and S^{iso} denotes the entanglement entropy in isotropic phase whereas S^{aniso} denotes that in anisotropic phase. We suggest a quantity $O_{12} \equiv S_1 - S_2$ as a new order parameter near the critical point, where S_1 is entanglement entropy when the slab is perpendicular to the direction of the vector order whereas S_2 is that when the slab is parallel to the vector order. $O_{12} = 0$ in isotropic phase but in anisotropic phase, the order parameter becomes non-zero showing the same scaling behavior. Finally, we show that even near the critical point, the first law of entanglement entropy is held. Especially, we find that the entanglement temperature for the cylinder is $\mathcal{T}_{cy} = \frac{c_{\text{ent}}}{a}$, where $c_{\text{ent}} = 0.163004 \pm 0.000001$ and a is the radius of the cylinder.

KEYWORDS: AdS-CFT Correspondence, Gauge-Gravity Correspondence, Holography and Hydrodynamics

ARXIV EPRINT: [2210.08919](https://arxiv.org/abs/2210.08919)

*Corresponding author.

Contents

| | | |
|----------|---|-----------|
| 1 | Introduction | 1 |
| 2 | Holographic model | 5 |
| 3 | Holographic computations of entanglement entropy of wide and thin slabs | 8 |
| 3.1 | The slab on $x_2 - x_3$ plane | 8 |
| 3.2 | The slab on $x_1 - x_3$ plane | 11 |
| 3.3 | Properties of holographic entanglement entropy near critical point | 13 |
| 4 | Holographic computation of entanglement entropy of a long cylinder with its radius, a and its length, L_1 along x_1-direction | 16 |
| 4.1 | Holographic entanglement calculation of cylinder | 16 |
| 4.2 | Evaluation of surface area and subtraction of UV-divergence | 19 |
| 5 | Discussion | 21 |
| A | Slabs on the x_2-x_3 and x_3-x_1 planes | 23 |
| A.1 | Slab on AdS boundary and divergence subtraction | 24 |
| A.2 | Slab on the x_2 - x_3 plane | 25 |
| A.3 | Slab on the x_3 - x_1 plane | 27 |
| B | Equations and solutions for the long cylinder | 28 |
| B.1 | Solutions for $z_0(\rho)$, $z^{(\alpha)}(\rho)$ and $z^{(\varepsilon)}(\rho)$ | 28 |
| B.2 | Black brane solution and entanglement temperature | 30 |
| B.3 | Computation of the surface area for cylinder | 31 |

1 Introduction

AdS/CFT correspondence has shed light on strongly coupled field theories by employing their holographic dual gravity theories [1–3]. Especially, fluid-gravity duality [4–6] and AdS-condensed matter theory(AdS/CMT) [10–12, 14] are widely studied in many literatures to explore low energy(long wavelength) limits of conformal field theories, which become conformal fluids, condensed matter systems and so on. Especially, in fluid-gravity duality, holographic computation of the ratio of shear viscosity, η to entropy density, \mathcal{S} is the most remarkable example and it is known to be universal, which is given by $\frac{\eta}{\mathcal{S}} = \frac{1}{4\pi}$ [4, 6–9].

An interesting issue related to fluid-gravity duality and AdS/CMT is thermodynamic phase transition where the system shows symmetry breaking because of emergence of an order parameter, a condensation. In condensed matter theory, electron-electron bound

states, so called Cooper pairs, are present near its critical point which breaks U(1) gauge symmetry of electrons.

A noticeable construction of gravity model for holographic condensed matter theory is based on a theory with complex scalar field defined in the background of (asymptotically AdS) charged black brane. [10, 12]. When the black brane temperature becomes below a certain critical temperature, $T = T_c$, the complex scalar field becomes unstable and condensed. The charged black brane geometry presents scalar hair due to this condensation. The condensation corresponds to U(1)-symmetry breaking due to emergence of a scalar order in the dual field theory system, and which implies super-conductor/normal-conductor phase transition.

It is also interesting to consider the emergence of vector(p-wave) or tensor(d-wave) order near the critical point. An interesting holographic model to explore p-wave superfluid/normal-fluid phase transition is Einstein-SU(2)Yang-Mills theory in asymptotically AdS₅ spacetime [13, 18–20]. A precise solution in the theory is a 5-dimensional charged black brane solution. In the solution, temporal direction of the Yang-Mills fields is turned on, which is proportional to $\tau_3 = \frac{\sigma_3}{2}$, where τ_3 is the third generator in SU(2) gauge group, σ_i are the Pauli-matrices and $i = 1, 2, 3$.

In this dual gravity model, for a certain chemical potential μ_c , an interesting mode of solution appears. This mode is the spatial component of Yang-Mills fields being proportional to $\tau_1 = \frac{\sigma_1}{2}$ and it is a normalizable mode of the solution. In fact, the black brane geometry enjoys SO(3)-global rotational symmetry mixing 3-dimensional spatial coordinates, $\{x_1, x_2, x_3\}$. However, once the spatial mode of solution appears, the SO(3) rotational symmetry is broken down to SO(2), where the direction of the spatial mode is chosen to be in x_1 -axis. In holographic dictionary, normalizable mode of solution in dual gravity corresponds to a state in the boundary field theory. Therefore, the symmetry is broken due to a state in the dual field theory and so it is spontaneous symmetry breaking(SSB).

One of the previous works to explore this SSB near the critical point is a study on the ratio of shear viscosity to entropy density in fluid-gravity duality [17, 18]. The shear viscosity defined in $x_2 - x_3$ plane, η_{23} retains its universal value of the ratio since SO(2)-rotational symmetry still exists whereas that defined in the plane which contains x_1 coordinate(e.g. η_{12}) will give the deviation from the universal value.

To study this holographic fluid system, one can apply either numerical or analytic methods. In [17], the authors consider numerical method and find out that when $\alpha = \frac{\kappa_5}{g}$ is less than a certain critical value, α_{crit} , the boundary fluid system shows second order phase transition whereas if α is greater than α_{crit} , it presents first order phase transition, where κ_5 is 5-dimensional gravity constant and g is the gauge coupling of the Yang-Mills fields. They also figure out that the deviation of the ratio from the universal value shows scaling behaviors near the critical point, such as

$$1 - 4\pi \frac{\eta_{12}}{S} \sim \left(1 - \frac{T}{T_c}\right)^\beta \tag{1.1}$$

and its critical exponent β is

$$\beta = 1.00 \pm 0.03, \tag{1.2}$$

where T is the charged black brane temperature, and T_c is critical temperature.

To determine the critical exponent more precisely, the authors in [18] employ analytic approach in large gauge coupling limit, $\alpha \ll 1$, together with the magnitude of spatial component of Yang-Mills fields, $\varepsilon \ll 1$ is small. The deviation is given by

$$1 - 4\pi \frac{\eta_{12}}{\mathcal{S}} = \frac{1305\pi T_c}{544} \left(1 - \frac{T}{T_c}\right)^\beta. \tag{1.3}$$

It turns out that the critical exponent is determined to be $\beta = 1$ in this analytic approach.

The analytic approach given in [18] to obtain such a deviation of the ratio of shear viscosity to entropy density is crucially based on their methodology of double expansion with parameters, α and ε in the bulk. The authors in [18] assume that the magnitude of the vector order, ε is small and so its subleading corrections are suppressed by ε . To get analytic form of the leading backreactions from the energy momentum tensor of the Yang-Mills fields, they also assume that α is small otherwise it is very unlikely to get the analytic solutions of the back reactions. This approach allows them to obtain the analytic form of the backreactions perturbatively. The leading corrections to the background geometry is $O(\varepsilon^2\alpha^2)$ and the subleading corrections are $O(\varepsilon^{1+i}\alpha^{2j})$, where i, j are positive integers and $i > 1$ or $j > 1$. We note that since this analytic approach is based on small α expansion, it is manifest that the thermodynamic phase transition observed in that analytic approach is second order one.

On the other hand, there is another interesting direction to explore the field theory system, (holographic) entanglement entropy. Entanglement entropy, which describes quantum correlation between a macroscopic subsystem and its complement, is one of the important quantities specifying quantum nature of a system. Based on the AdS/CFT correspondence, Ryu and Takayanagi propose that the entanglement of a quantum field theory can be evaluated by calculating the area of a minimal surface extending to the dual geometry [15, 16] and it is further developed in [21, 22]. This provides more precise understanding between gravity theory in asymptotically AdS space and the dual field theory defined on its conformal boundary [23].

Especially, an interesting property of (holographic) entanglement entropy is that there is a concrete relation between the subsystem energy and its entanglement entropy in the limit that the system size is very much small, which is called the first law of entanglement entropy [24–33]. In small subsystem limit, there is a relation, $\Delta E = \mathcal{T}\Delta S$, where ΔE is energy difference of the subsystem when it is excited and ΔS is the corresponding change of the entanglement entropy. \mathcal{T} is called entanglement temperature. We note that it is widely discussed that the entanglement temperature is universally proportional to the inverse of the subsystem size regardless of the shape and dimensionality of the entangling region.

In this paper, we study Einstein SU(2) Yang-Mills theory near critical point, by employing holographic entanglement entropy. In the dual field theory, a vector order appears and it breaks SO(3) rotational symmetry. Especially, we concentrate on some features of (holographic) entanglement entropy near critical point as follows. One may expect that

entanglement entropy will perceive some of thermodynamic properties of field theory system near critical point. Since the gravity model undergoes second order phase transition near critical point, one may wonder if (holographic) entanglement entropy may show a scaling behavior like other quantities such as η_{12} , the ratio of shear viscosity to entropy density in anisotropic direction. Another question is if entanglement entropy can provide a new order parameter like the vector order parameter that we discuss above. From this, one can recognize that the $SO(3)$ spatial rotational symmetry breaks down to $SO(2)$. Finally, we want to check if the first law of entanglement entropy near the critical point is still valid, keeping its universal properties of entanglement temperature, even though the $SO(3)$ symmetry is broken by the vector order.

In the following, we will answer the questions that we raised above in order. First of all, we compute entanglement entropies of subsystems on the boundary spacetime with shapes of “wide and thin slabs” and a “cylinder”. The slabs are computable examples by applying analytic approaches¹ but for the cylinder case, we need numerics as well as analytic ones.² We study two different slabs, which share the same shape but we put them in different directions. More precisely, we consider a wide slab which is perpendicular to the vector order (the vector order is along x_1 -direction) and another slab being parallel to the vector order. We call each of the entanglement entropy S_1, S_2 respectively. We define quantities, $\Delta_\varepsilon S_i \equiv S_i^{\text{iso}} - S_i^{\text{aniso}}$ ($i = 1, 2$), which shows how much the excess of entanglement entropy is when the boundary field theory system shows phase transition to anisotropic phase from isotropic phase. It turns out that $\Delta_\varepsilon S_i$ presents a scaling behavior such that

$$\Delta_\varepsilon S_i = \frac{2520\pi^2}{17\kappa_5^2} \Sigma_i \mathcal{A}_i^{(\varepsilon)}(d) T_c \left(1 - \frac{T}{T_c}\right)^\beta, \tag{1.4}$$

where the critical exponent β turns out to be one, i.e. $\beta = 1$. Σ_i is the cross sectional area of each slab, $\mathcal{A}_i^{(\varepsilon)}$ are the factors, showing “ d ” dependence, where d is the thickness of the slabs and T_c is the critical temperature. The leading behaviors of $\mathcal{A}_i^{(\varepsilon)}$ is given by

$$\mathcal{A}_i^{(\varepsilon)}(d) = \frac{281}{134400\pi^{7/2}} \Gamma\left(\frac{1}{3}\right)^3 \Gamma\left(\frac{1}{6}\right)^3 d^2 + O(d^4), \tag{1.5}$$

for both of $\mathcal{A}_i^{(\varepsilon)}$ but the next sub-leading is different from each other. For the subsystem with its shape of cylinder, we also compute the same quantity, $\Delta_\varepsilon S_{cy} = S_{cy}^{\text{iso}} - S_{cy}^{\text{aniso}}$ as we discussed above and find that

$$\Delta_\varepsilon S_{cy} = \frac{5040\pi^2 L_1}{17\kappa_5^2} \gamma^{(\varepsilon)}(a) T_c \left(1 - \frac{T}{T_c}\right)^\beta, \tag{1.6}$$

where

$$\gamma^{(\varepsilon)}(a) = 0.163313a^3 + O(a^4), \tag{1.7}$$

¹We note that there are some of earlier numerical works [42, 43], in which they discuss entanglement entropy of a slab in this background.

²We get analytic(algebraic) solutions of surface area for the cylinder on AdS boundary. To apply one of the boundary conditions to the surface, we use numerics. For the details, see section 4.1.

where a and L_1 is the radius and the length of the cylinder and $\beta = 1$. We note that to get this results, we utilize analytic as well as numerical methods.

Second of all, once we set the cross-sectional area of the two slabs to be equal as $\Sigma \equiv \Sigma_1 = \Sigma_2$, we can define an interesting new order parameter $\mathcal{O}_{12} \equiv S_1 - S_2$ which vanishes in isotropic phase. However, once the dual field theory system gets into the anisotropic phase, it becomes

$$\mathcal{O}_{12} = S_1^{\text{aniso}} - S_2^{\text{aniso}} = -\frac{2520\pi^2}{17\kappa_5^2} \Sigma \mathcal{A}^{(\varepsilon)}(d) T_c \left(1 - \frac{T}{T_c}\right)^\beta, \quad (1.8)$$

which also shows the same critical exponent $\beta = 1$. The leading behavior of $\mathcal{A}^{(\varepsilon)}(d)$ is proportional to $\sim d^4$. More precisely, the leading behavior of $\mathcal{A}^{(\varepsilon)}(d)$ is given by

$$\mathcal{A}^{(\varepsilon)}(d) = \frac{3\sqrt{3}}{448\pi^{9/2}} \Gamma\left(\frac{1}{6}\right)^3 \Gamma\left(\frac{1}{3}\right)^3 d^4 + O(d^6). \quad (1.9)$$

Finally, we study the first law of entanglement entropy in this framework. We find that even in the case that the vector order appears near critical point, the first law of entanglement entropy is still valid for both of the subsystems of the slabs and the cylinder. This means that subsystem energy and entanglement entropy are proportional to each other and the ratio of one to another is the same \mathcal{T} , which is the entanglement temperature when the subsystem is out of the critical point. Especially, by employing analytic as well as numerical methods, we determine entanglement temperature of the subsystem with the shape of cylinder, which is given by

$$\mathcal{T}_{cy} = \frac{c_{\text{ent}}}{a}, \quad \text{where } c_{\text{ent}} = 0.163004 \pm 0.000001, \quad (1.10)$$

where a is the radius of the cylinder.

We close this section with a remark. The critical behaviors and the fact that its critical exponent $\beta = 1$ of the entanglement entropies are turned out to be universal features in our analytic approach. However, anisotropic features also appear in the factors, for example, $\mathcal{A}_i^{(\varepsilon)}(d)$ in thin and wide slab cases. In the small “ d ” region, we only see the leading behavior of entanglement entropy which is proportional to d^2 . However, as d increases, the subleading corrections become important and it shows spatial anisotropy and it may depend on an angle between the direction of the vector order and the axis that the slab is lying in. Our analysis manifestly shows that the leading behaviors of the anisotropy in the entanglement entropy is contained the coefficient, $\mathcal{A}_i^{(\varepsilon)}(d)$, which have information of directional dependency of degrees of freedom when the vector order appears.

2 Holographic model

In this section, we will review the holographic model for anisotropic super fluids defined on its conformal boundary. To illustrate the model, we mostly follow the papers [18, 19]. We begin with the holographic model given by

$$S = \int d^5x \sqrt{-G} \left(\frac{1}{\kappa_5^2} \left(R + \frac{12}{L^2} \right) - \frac{1}{4g^2} F_{MN}^a F^{aMN} \right), \quad (2.1)$$

where κ_5 is 5-dimensional gravity constant, g is the gauge coupling for SU(2) gauge field B_M^a . L is the length scale for cosmological constant and we set $L = 1$ in the following discussion. The field strength for the gauge fields is given by

$$F_{MN}^a = \partial_M B_N^a - \partial_N B_M^a - \varepsilon^{abc} B_M^b B_N^c, \quad (2.2)$$

where indices with upper case Latin letters as M, N, \dots are spacetime indices and the indices with the lower case Latin letters are gauge indices, and they run as $a, b, c = 1, 2, 3$. ε^{abc} is fully anti-symmetric tensor.

By applying variational principle of the fields to the action, we get their equations of motion. They are

$$W_{MN} \equiv R_{MN} + 4G_{MN} - \kappa_5^2 \left(T_{MN} - \frac{1}{3} T_P^P G_{MN} \right) = 0, \quad (2.3)$$

$$Y^{aN} \equiv \nabla_M F^{aMN} - \varepsilon^{abc} B_M^b F^{cMN} = 0, \quad (2.4)$$

where W_{MN} is Einstein equation and Y_M^a is gauge field equation. T_{MN} is stress-energy tensor being given by

$$T_{MN} = \frac{1}{g^2} \left(F_{MP}^a F_N^{Pa} - \frac{1}{4} F_{PQa} F^{PQa} G_{MN} \right). \quad (2.5)$$

Now, we are going to get their solutions. The forms of the solutions that we try are

$$B = \phi(r)\tau^3 dt + \omega(r)\tau^1 dx_1, \quad (2.6)$$

$$ds^2 = -N(r)\sigma^2(r)dt^2 + \frac{dr^2}{N(r)} + r^2 f^{-4}(r)dx_1^2 + r^2 f^2(r)(dx_2^2 + dx_3^2), \quad (2.7)$$

where x_1, x_2 , and x_3 are the boundary spatial coordinates. One of the solutions is 5-dimensional charged black brane solution, which is given by

$$\phi(r) = \mu \left(1 - \frac{1}{r^2} \right), \quad \omega(r) = 0, \quad (2.8)$$

$$\sigma(r) = f(r) = 1 \text{ and } N(r) = N_0(r) \equiv r^2 - \frac{m}{r^2} + \frac{2\mu^2\alpha^2}{3r^4},$$

where μ is chemical potential for the gauge field ϕ , $m = 1 + \frac{2\mu^2\alpha^2}{3}$ is the mass of the black brane and the constant $\alpha^2 \equiv \frac{\kappa_5^2}{g^2}$. We note that the horizon of the black brane is located at $r = 1$ in this solution by employing an appropriate coordinate rescaling such that $r \rightarrow \lambda r$ and $\{t, x_1, x_2, x_3\} \rightarrow \lambda^{-1}\{t, x_1, x_2, x_3\}$ with a real constant λ . In this rescaled coordinate, the chemical potential μ is dimensionless and it turns out that at $\mu = 4$, the normalizable mode of solution $\omega(r)$ appears.

Now, we are interested in another kind of solutions, where $\omega(r)$ does not vanish. The way how to get a solution is to solve the gauge field equations (2.4) by assuming that the $\omega(r)$ is non-zero but still small. It turns out that the form of the solution $\omega(r)$ is given by

$$\omega(r) = \varepsilon \frac{r^2}{(r^2 + 1)^2} + O(\varepsilon^2), \quad (2.9)$$

where ε is a small parameter representing the magnitude of $\omega(r)$.

The solution $\omega(r)$ is x_1 -directional gauge field, which breaks $SO(3)$ global rotation symmetry of the spacetime into $SO(2)$. This becomes more manifest when we compute back reactions to the black brane background spacetime. To compute backreactions, we assume the α^2 is also parametrically small and so stress-energy tensor of the gauge field excitation, $\phi(r)$ and $\omega(r)$ does not significant change the background. We briefly list the results below considering backreactions to the field ϕ upto leading order in ε^2 and the background spacetime upto leading order in $\varepsilon^2\alpha^2$.

$$\omega(r) = \varepsilon \frac{r^2}{(r^2 + 1)^2} + O(\varepsilon^2), \tag{2.10}$$

$$\phi(r) = 4 \left(1 - \frac{1}{r^2}\right) + \frac{\varepsilon^2}{4} \left(\frac{1 + 2r^2}{3r^2(1 + r^2)^3} - \frac{1}{8} + \frac{281}{1680} \left(1 - \frac{1}{r^2}\right) \right) + O(\varepsilon^3) \tag{2.11}$$

and

$$\begin{aligned} \sigma(r) &= 1 - \varepsilon^2\alpha^2 \frac{2}{9(1+r^2)^3}, \quad f(r) = 1 - \varepsilon^2\alpha^2 F(r) \tag{2.12} \\ N(r) &= N_0(r) \left(1 - \alpha^2 N_\alpha(r) + \varepsilon^2\alpha^2 N_\varepsilon(r)\right) \end{aligned}$$

where

$$F(r) = \frac{1}{18} \frac{1 - 2r^2}{(1 + r^2)^4}, \tag{2.13}$$

$$N_0(r) = r^2 - \frac{1}{r^2}, \quad N_\alpha = \frac{32}{3} \frac{1}{r^2(r^2 + 1)}, \quad \text{and} \quad N_\varepsilon(r) = \frac{4}{9} \frac{1}{r^2} \left(\frac{281}{560} \frac{1}{r^2} - \frac{2 + 6r^2 + 3r^4}{2(1 + r^2)^4} \right) \tag{2.14}$$

Sometimes, we employ the radial coordinate z , which is defined by $z = \frac{1}{r}$. In such a case, the metric is

$$ds^2 = \frac{1}{z^2} \left\{ -z^2 N(z) \sigma^2(z) dt^2 + \frac{dz^2}{z^2 N(z)} + f^{-4}(z) dx_1^2 + f^2(z) (dx_2^2 + dx_3^2) \right\}, \tag{2.15}$$

where,

$$\begin{aligned} f(z) &= 1 - \varepsilon^2\alpha^2 F(z), \tag{2.16} \\ N(z) &= N_0(z) \left(1 - \alpha^2 N_\alpha(z) - \varepsilon^2\alpha^2 N_\varepsilon(z)\right). \end{aligned}$$

and

$$F(z) = \frac{1}{18} \frac{z^6(z^2 - 2)}{(z^2 + 1)^4}, \tag{2.17}$$

$$N_0(z) = \frac{1}{z^2} - z^2, \quad N_\alpha(z) = \frac{32}{3} \frac{z^4}{1 + z^2}, \quad \text{and} \quad N_\varepsilon(z) = \frac{4}{9} z^4 \left(\frac{281}{560} - \frac{2z^6 + 6z^4 + 3z^2}{2(1 + z^2)^4} \right) \tag{2.18}$$

Finally, we discuss some of the black brane thermodynamics. The black brane temperature is given by

$$T = \frac{1}{\pi} \left(1 - \frac{16}{3}\alpha^2 + \frac{17}{1260}\varepsilon^2\alpha^2 \right) \tag{2.19}$$

and the black brane entropy is

$$S_{\text{black-brane}} = \frac{2\pi}{\kappa_5^2} V_3, \tag{2.20}$$

where we take the horizon located at $z = 1$ and V_3 is the spatial coordinate volume, $V_3 = \int d^3\vec{x}$. We note that the critical temperature, T_c is given by

$$T_c = \frac{1}{\pi} \left(1 - \frac{16}{3}\alpha^2 \right). \tag{2.21}$$

3 Holographic computations of entanglement entropy of wide and thin slabs

In this section, we will discuss holographic entanglement entropy probes near critical point, $T = T_c$ in the presence of the vector mode $\omega(r)$ and considering its backreaction to the background geometry. We consider a subsystem on AdS boundary with its shape of wide slab. There are two different ways to put the slab, which are to put that on $x_2 - x_3$ plane and on $x_3 - x_1$ plane (remember that x_1 - direction is parallel to the vector order $\omega(r)$).

3.1 The slab on $x_2 - x_3$ plane

Think of a slab on AdS boundary where the slab is given by $-\frac{L_2}{2} \leq x_2 \leq \frac{L_2}{2}$, $-\frac{L_3}{2} \leq x_3 \leq \frac{L_3}{2}$ and $-\frac{d}{2} \leq x_1 \leq \frac{d}{2}$. We take L_2 and L_3 to be very large, which makes the subsystem have translational symmetric directions along x_2 and x_3 axes ($L_2, L_3 \rightarrow \infty$). Now we compute a surface area in $d + 1$ -dimensional bulk from the slab on AdS boundary, which is given by

$$A_1 = \lim_{\delta \rightarrow 0} 2L_2L_3 \int_{r_*}^{\frac{1}{\delta}} dr r^3 \sqrt{\frac{f^4(r)}{r^2 N(r)} + \left(\frac{dx_1}{dr}\right)^2}, \tag{3.1}$$

where boundary of the surface, A_1 (located at $r = \frac{1}{\delta}$ together with $\delta \rightarrow 0$) matches with the boundary of the slab on AdS boundary. A_1 is hanged down into the bulk and there is a minimum value of the radial variable, r . We address that minimum value as r_* .

Holographic entanglement entropy, S is related to the area of surface in the bulk, A as

$$S = \frac{2\pi}{\kappa^2} A, \tag{3.2}$$

where A needs to be minimized followed by Ryu-Takayanagi-prescription [15, 16]. To extremize the surface, we apply variational principle to the area and we get the condition of extremum being given as

$$\frac{d}{dr} \left(r^3 \frac{x_1'}{\sqrt{(x_1')^2 + \frac{f^4(r)}{r^2 N(r)}}} \right) = 0, \tag{3.3}$$

where the prime denotes derivative with respect to r . Let us close look at the inside the round bracket in (3.3). The A_1 is hanged down deep into the bulk spacetime and it becomes deepest when $\frac{dr}{dx_1} = 0$ and it is given when $x_1 = 0$. The solution of equation (3.3) is that the quantity inside of round bracket is a constant and the above argument fixes the constant as $r^3 \frac{x_1'}{\sqrt{(x_1')^2 + \frac{f^4(r)}{r^2 N(r)}}} = r_*^3$.

With such an identification, the solution is able to be written as

$$x_1' = \pm \frac{r_*^3 f^2(r)}{r^4 \sqrt{\left(1 - \frac{r_*^6}{r^6}\right) N(r)}}, \tag{3.4}$$

and we substitute the solution into the surface area A_1 to remove $\frac{dx_1}{dr}$ in it. Then, A_1 is given by

$$A_1 = 2L_2 L_3 \lim_{\delta \rightarrow 0} \int_{r_*}^{\frac{1}{\delta}} dr \frac{r^2 f^2(r)}{\sqrt{N(r)}} \left(1 - \frac{r_*^6}{r^6}\right)^{-\frac{1}{2}}. \tag{3.5}$$

Moreover, between r_* and d (the thickness of the slab lying in the x_1 -direction), there is the following relationship:

$$d = 2 \lim_{\delta \rightarrow 0} \int_{r_*}^{\frac{1}{\delta}} \frac{dr}{\sqrt{\frac{r^2 N(r)}{f^4(r)} \left(\frac{r^6}{r_*^6} - 1\right)}}, \tag{3.6}$$

which can be easily derived by using an identity, $\int_{-d/2}^{d/2} dx_1 = 2 \lim_{\delta \rightarrow 0} \int_{r_*}^{\frac{1}{\delta}} \frac{dr(x_1)}{r'(x_1)}$, where the prime denotes that the derivative with respect to its argument.

To evaluate the integration for the surface area, A_1 given in (3.5), we need to look at the metric factors, $N(r)$ and $f(r)$ in (2.12) carefully. The metric is obtained by taking into account backreactions from the vector order $\omega(r)$ upto its leading order corrections. The leading correction is order of $\varepsilon^2 \alpha^2$. We note again that $\alpha^2 = \frac{\kappa^2}{g^2}$ is regarded as small parameter as well as $\varepsilon^2 \ll 1$ and we deal with those perturbatively. In sum, we expand the surface area A_1 upto leading order correction in $\varepsilon^2 \alpha^2$ and evaluate the integrations. Then, we have α^2 and ε^2 corrections together with the zeroth order terms in α and ε in A_1 . Each integration is not so easy to get an analytic and compact form, so we assume that d is small as well as $r_* \gg 1$ to get a series form of the integrands in small d . Firstly, by applying all the arguments that we address above, we evaluate the relation (3.6), which is given by

$$d = \frac{2\sqrt{\pi} \Gamma\left(\frac{2}{3}\right)}{\Gamma\left(\frac{1}{6}\right)} \frac{1}{r_*} + \frac{\sqrt{\pi} \Gamma\left(\frac{4}{3}\right) (1260 + 13440\alpha^2 + 281\alpha^2\varepsilon^2)}{7560 \Gamma\left(\frac{11}{6}\right)} \left(\frac{1}{r_*}\right)^5 - \frac{\sqrt{\pi} \Gamma\left(\frac{5}{3}\right) (4480\alpha^2 + 187\alpha^2\varepsilon^2)}{2520 \Gamma\left(\frac{13}{6}\right)} \left(\frac{1}{r_*}\right)^7 \dots, \tag{3.7}$$

and its inverse relation is

$$\frac{1}{r_*} = \frac{\Gamma\left(\frac{1}{6}\right)}{2\sqrt{\pi}\Gamma\left(\frac{2}{3}\right)} d - \frac{\Gamma\left(\frac{1}{6}\right)^6 \Gamma\left(\frac{4}{3}\right) (1260 + 13440\alpha^2 + 281\alpha^2\varepsilon^2)}{483840 \pi^{5/2} \Gamma\left(\frac{2}{3}\right)^6 \Gamma\left(\frac{11}{6}\right)} d^5 + \frac{\Gamma\left(\frac{1}{6}\right)^8 \Gamma\left(\frac{5}{3}\right) (4480\alpha^2 + 187\alpha^2\varepsilon^2)}{645120 \pi^{7/2} \Gamma\left(\frac{2}{3}\right)^8 \Gamma\left(\frac{13}{6}\right)} d^7 \dots \tag{3.8}$$

Now, we evaluate the minimal surface area A_1 by replacing r_* in it with d by using the above relation together.

In fact, A_1 contains divergence which depends on the radial cut-off, $\frac{1}{\delta}$ near AdS boundary. This divergence already appears in entanglement entropy computation in pure AdS background, and we call that $S_1^{(AdS)}$. Therefore, we need to define a renormalized entanglement entropy, where we define the renormalized version of entanglement entropy as

$$S_1^{(\text{ren})} = S_1 - S^{(AdS)}. \tag{3.9}$$

It turns out that the entanglement entropy in AdS background is given by

$$S^{(AdS)} = \frac{2\pi}{\kappa_5^2} \Sigma_1 A^{(AdS)}, \tag{3.10}$$

where Σ_1 is the coordinate volume of the slab,

$$\Sigma_1 = L_2 L_3. \tag{3.11}$$

The $A^{(AdS)}$ is given by

$$A^{(AdS)} = \lim_{\delta \rightarrow 0} \frac{1}{\delta^2} - \frac{32\pi^{9/2}}{3\sqrt{3}\Gamma\left(\frac{1}{3}\right)^3 \Gamma\left(\frac{1}{6}\right)^3} d^{-2}, \tag{3.12}$$

which contains the divergence appearing near AdS boundary and the finite term being proportional to d^{-2} . Now, we will subtract this quantity from S_1 , and we get the renormalized entanglement entropy, which is given by

$$S_1^{(\text{ren})} = \frac{2\pi}{\kappa_5^2} \Sigma_1 \mathcal{A}_1, \tag{3.13}$$

where \mathcal{A}_1 is

$$\mathcal{A}_1 = \mathcal{A}_1^{(0)} + \alpha^2 \mathcal{A}_1^{(\alpha)} + \varepsilon^2 \alpha^2 \mathcal{A}_1^{(\varepsilon)}, \tag{3.14}$$

and

$$\begin{aligned} \mathcal{A}_1^{(0)} &= \frac{3}{320\pi^{7/2}} \Gamma\left(\frac{1}{3}\right)^3 \Gamma\left(\frac{1}{6}\right)^3 d^2 \\ &+ \frac{27}{16384\pi^9} \Gamma\left(\frac{1}{3}\right)^6 \Gamma\left(\frac{1}{6}\right)^6 \left(1 - \frac{13\sqrt{3}}{1800\pi^{5/2}} \Gamma\left(\frac{1}{3}\right)^3 \Gamma\left(\frac{1}{6}\right)^3\right) d^6 + O(d^7), \end{aligned} \quad (3.15)$$

$$\begin{aligned} \mathcal{A}_1^{(\alpha)} &= \frac{1}{10\pi^{7/2}} \Gamma\left(\frac{1}{3}\right)^3 \Gamma\left(\frac{1}{6}\right)^3 d^2 - \frac{3\sqrt{3}}{28\pi^{9/2}} \Gamma\left(\frac{1}{3}\right)^3 \Gamma\left(\frac{1}{6}\right)^3 d^4 \\ &+ \frac{9}{256\pi^9} \Gamma\left(\frac{1}{3}\right)^6 \Gamma\left(\frac{1}{6}\right)^6 \left(1 - \frac{13\sqrt{3}}{1800\pi^{5/2}} \Gamma\left(\frac{1}{3}\right)^3 \Gamma\left(\frac{1}{6}\right)^3\right) d^6 + O(d^7), \end{aligned} \quad (3.16)$$

$$\begin{aligned} \mathcal{A}_1^{(\varepsilon)} &= \frac{281}{134400\pi^{7/2}} \Gamma\left(\frac{1}{3}\right)^3 \Gamma\left(\frac{1}{6}\right)^3 d^2 - \frac{561\sqrt{3}}{125440\pi^{9/2}} \Gamma\left(\frac{1}{3}\right)^3 \Gamma\left(\frac{1}{6}\right)^3 d^4 \\ &- \frac{837}{1146880\pi^9} \Gamma\left(\frac{1}{3}\right)^6 \Gamma\left(\frac{1}{6}\right)^6 \left(1 + \frac{3653\sqrt{3}}{502200\pi^{5/2}} \Gamma\left(\frac{1}{3}\right)^3 \Gamma\left(\frac{1}{6}\right)^3\right) d^6 + O(d^7). \end{aligned} \quad (3.17)$$

3.2 The slab on $x_1 - x_3$ plane

To put the slab on the $x_1 - x_3$ plane, we parametrize the slab as $-\frac{L_3}{2} \leq x_3 \leq \frac{L_3}{2}$, $-\frac{L_1}{2} \leq x_1 \leq \frac{L_1}{2}$ and $-\frac{d}{2} \leq x_2 \leq \frac{d}{2}$. Again, we take L_1 and L_3 to be very large, meaning that we take a parametric limit as L_1 and $L_3 \rightarrow \infty$. The formula for the surface area hanged down in the bulk is given by

$$A_2 = L_1 L_3 \lim_{\delta \rightarrow 0} \int_{r_{\#}}^{1/\delta} dr r^3 \sqrt{\frac{1}{r^2 f^2(r) N(r)} + \left(\frac{dx_2}{dr}\right)^2}, \quad (3.18)$$

and its equation for extremum is

$$\frac{d}{dr} \left(r^3 \frac{x'_2}{\sqrt{(x'_2)^2 + \frac{1}{r^2 f^2(r) N(r)}}} \right) = 0, \quad (3.19)$$

where again the boundary of the surface area, A_2 is coincide with the boundary of the slab at $r = \frac{1}{\delta}$ where we take a limit of $\delta \rightarrow 0$. We also define $r_{\#}$ this time, which is the minimum of the r -value. By applying the similar argument that we addressed in the case with slab lying on $x_1 - x_2$ plane, we get

$$x'_2 = \pm \frac{r_{\#}^3}{r^4 f(r) \sqrt{\left(1 - \frac{r_{\#}^6}{r^6}\right) N(r)}}. \quad (3.20)$$

Now, we plug the solution of the equation of extremum (3.20) into the expression of the surface area A_2 (3.18), we get

$$A_2 = 2L_1 L_3 \lim_{\delta \rightarrow 0} \int_{r_{\#}}^{1/\delta} dr \frac{r^2}{f(r) \sqrt{N(r)}} \left(1 - \frac{r_{\#}^6}{r^6}\right)^{-\frac{1}{2}}. \quad (3.21)$$

We also get the relation between the minimum value of r , $r_{\#}$ and d in this case too. The form of the expression is

$$d = 2 \lim_{\delta \rightarrow 0} \int_{r_{\#}}^{\frac{1}{\delta}} \frac{dr}{\sqrt{r^2 N(r) f^2(r) \left(\frac{r^6}{r_{\#}^6} - 1 \right)}}. \quad (3.22)$$

and its final form after performing the integration in it is given by

$$d = \frac{2\sqrt{\pi} \Gamma\left(\frac{2}{3}\right)}{\Gamma\left(\frac{1}{6}\right)} \frac{1}{r_{\#}} + \frac{\sqrt{\pi} \Gamma\left(\frac{4}{3}\right) (1260 + 13440\alpha^2 + 281\alpha^2\varepsilon^2)}{7560 \Gamma\left(\frac{11}{6}\right)} \left(\frac{1}{r_{\#}}\right)^5 - \frac{\sqrt{\pi} \Gamma\left(\frac{5}{3}\right) (4480\alpha^2 + 467\alpha^2\varepsilon^2)}{2520 \Gamma\left(\frac{13}{6}\right)} \left(\frac{1}{r_{\#}}\right)^7 \dots \quad (3.23)$$

The inverse relation of this is

$$\frac{1}{r_{\#}} = \frac{\Gamma\left(\frac{1}{6}\right)}{2\sqrt{\pi} \Gamma\left(\frac{2}{3}\right)} d - \frac{\Gamma\left(\frac{1}{6}\right)^6 \Gamma\left(\frac{4}{3}\right) (1260 + 13440\alpha^2 + 281\alpha^2\varepsilon^2)}{483840 \pi^{5/2} \Gamma\left(\frac{2}{3}\right)^6 \Gamma\left(\frac{11}{6}\right)} d^5 + \frac{\Gamma\left(\frac{1}{6}\right)^8 \Gamma\left(\frac{5}{3}\right) (4480\alpha^2 + 467\alpha^2\varepsilon^2)}{645120 \pi^{7/2} \Gamma\left(\frac{2}{3}\right)^8 \Gamma\left(\frac{13}{6}\right)} d^7 \dots \quad (3.24)$$

Together with the relation (3.24) and the expression of A_2 given in (3.21), the holographic entanglement entropy is given by

$$S_2^{(\text{ren})} = \frac{2\pi}{\kappa_5^2} \Sigma_2 \mathcal{A}_2, \quad (3.25)$$

where $S_2^{(\text{ren})} = S_2 - S^{(AdS)}$ and Σ_2 represents $\Sigma_2 = L_1 L_3$. We note that again to evaluate the integration in the expression, A_2 , we expand that upto leading order in α^2 and $\varepsilon^2\alpha^2$ together with $\frac{1}{r_{\#}}$ expansion with an assumption that $r_{\#} \gg 1$ and $d \ll 1$.

The \mathcal{A}_2 is also defined as the similar fashion as we did in the previous computation, being given by

$$\mathcal{A}_2 = \mathcal{A}_2^{(0)} + \alpha^2 \mathcal{A}_2^{(\alpha)} + \varepsilon^2 \alpha^2 \mathcal{A}_2^{(\varepsilon)}, \quad (3.26)$$

where

$$\mathcal{A}_2^{(0)} = \mathcal{A}_1^{(0)}, \quad \mathcal{A}_2^{(\alpha)} = \mathcal{A}_1^{(\alpha)} \quad (3.27)$$

and

$$\mathcal{A}_2^{(\varepsilon)} = \frac{281}{134400\pi^{7/2}} \Gamma\left(\frac{1}{3}\right)^3 \Gamma\left(\frac{1}{6}\right)^3 d^2 - \frac{1401\sqrt{3}}{125440\pi^{9/2}} \Gamma\left(\frac{1}{3}\right)^3 \Gamma\left(\frac{1}{6}\right)^3 d^4 - \frac{6723}{1146880\pi^9} \Gamma\left(\frac{1}{3}\right)^6 \Gamma\left(\frac{1}{6}\right)^6 \left(1 + \frac{3653\sqrt{3}}{4033800\pi^{5/2}} \Gamma\left(\frac{1}{3}\right)^3 \Gamma\left(\frac{1}{6}\right)^3\right) d^6 + O(d^7). \quad (3.28)$$

3.3 Properties of holographic entanglement entropy near critical point

Scaling behavior of entanglement entropy near critical point. As we discussed in section 1, this Einstein-SU(2)Yang-Mills system undergoes second order phase transition near the critical point, $T = T_c$, which is the phase transition from “isotropic phase” to “anisotropic phase” being affected by the appearance of vector order $\omega(r)$. Again, the $\omega(r)$ is the spatial component, B_1^1 of Yang-Mills fields, B_μ^a .

Now, we define the “isotropic” and the “anisotropic” phases as follows. In isotropic phase, $\omega(r) = 0$ and there is no backreaction to the background geometry from it. Since there is no spatial component of Yang-Mills fields turned on, the SO(3) isometry(spatial rotation symmetry) in the bulk spacetime is retained. However, once the field $\omega(r)$ is turned on, this spatial isometry is broken down to SO(2) and we call it anisotropic phase. The field $\omega(r)$ is normalizable mode in the bulk, which means that this mode corresponds to a state in dual field theory. We note that SO(3) isometry is broken spontaneously.

In many literatures [18–20], it is widely discussed that once $\omega(r)$ appears near critical point, the anisotropic phase is thermodynamically favored than the isotropic phase, and so there will be thermodynamic phase transition from isotropic phase to anisotropic phase, near the critical point.

The leading order backreaction from the field solution, $\omega(r)$ is order of $\varepsilon^2\alpha^2$ (Remember that $\omega(r) \sim \varepsilon$). Therefore, if we compute a quantity where we turn off $\varepsilon = 0$, then it corresponds to the quantity in isotropic phase whereas if we turn on ε and keep the leading order backreactions to the background geometry upto $\varepsilon^2\alpha^2$, then that quantity will be that in anisotropic phase. We call them Q^{iso} and Q^{aniso} respectively for some quantity, Q .

Now, we want see how much entanglement entropy excess arises, when the system undergoes phase transition. To see this, we define

$$\Delta_\varepsilon S_i \equiv S_i^{\text{iso}} - S_i^{\text{aniso}} = S_i^{(\text{ren})\text{iso}} - S_i^{(\text{ren})\text{aniso}}, \quad (3.29)$$

where $i = 1, 2$ to express, S_1 and S_2 respectively. We note that $\Delta_\varepsilon S_i$ is order of $\varepsilon^2\alpha^2 \sim \left(1 - \frac{T}{T_c}\right)$, which will show scaling behavior near the critical temperature $T = T_c$. In fact, by using black brane (critical)temperature (2.19) and (2.21), we get

$$\Delta_\varepsilon S_i = \frac{2520\pi^2}{17\kappa_5^2} \Sigma_i \mathcal{A}_i^{(\varepsilon)} T_c \left(1 - \frac{T}{T_c}\right)^\beta, \quad (3.30)$$

where β is the critical exponent of the entropy, and it turns out that

$$\beta = 1, \quad (3.31)$$

upto leading order corrections in α and ε in our analytic calculation.

Order parameter measuring spatial anisotropy from entanglement entropy. In fact, one can introduce a new order parameter near the critical point by employing (holographic) entanglement entropy. We define an order parameter of anisotropy near the critical point, being given by

$$O_{12} \equiv S_1 - S_2, \quad (3.32)$$

which denotes the difference of entanglement entropies between the slabs being perpendicular to the vector order, x_1 -direction and lying along the vector order. Once we make the cross section area of the slabs be the same, $\Sigma_1 = \Sigma_2 \equiv \Sigma$, then the quantity \mathcal{O}_{12} vanishes in isotropic phase. However, near the critical point, this quantity shows non-zero value such that

$$\mathcal{O}_{12} \equiv S_1^{\text{aniso}} - S_2^{\text{aniso}} = -\frac{2520\pi^2}{17\kappa_5^2} \Sigma \mathcal{A}^{(\varepsilon)} T_c \left(1 - \frac{T}{T_c}\right)^\beta, \quad (3.33)$$

where

$$\mathcal{A}^{(\varepsilon)} = \mathcal{A}_1^{(\varepsilon)} - \mathcal{A}_2^{(\varepsilon)} = \frac{3\sqrt{3}}{448\pi^{9/2}} \Gamma\left(\frac{1}{6}\right)^3 \Gamma\left(\frac{1}{3}\right)^3 d^4 + \frac{2943}{573440\pi^9} \Gamma\left(\frac{1}{6}\right)^6 \Gamma\left(\frac{1}{3}\right)^6 d^6 + O(d^7). \quad (3.34)$$

Again the critical exponent, $\beta = 1$ in our analytic analysis.

The leading dependence on the thickness of the slab, “ d ” in the order parameter, $\mathcal{O}_{12} \sim d^4$. The difference between S_1 and S_2 near the critical point stems from the $F(r)$ in the metric factor $f(r)$ which are given in (2.12) and (2.13). The reason why this happens is that $g_{11} \neq g_{22} = g_{33}$, which are the spatial components of bulk spacetime metric factors (See the metric (2.7)). The leading backreaction to the metric from the vector order, appears at $N_\varepsilon(r)$ in the metric factor $N(r)$, but $N_\varepsilon(r)$ does not give spatial anisotropy in the bulk spacetime metric. In fact, $N_\varepsilon(r) \sim O(r^{-4})$, whereas the metric factor $F(r) \sim O(r^{-6})$. Therefore, $F(r)$ gives subleading correction as contrasted with $N_\varepsilon(r)$ correction once we consider near AdS boundary expansion order by order in small $1/r_*$ or $1/r_\#$. However, Once we think of $\mathcal{O}_{12} = S_1 - S_2$, then contributions from $F(r)$ becomes leading, it grows as the subsystem becomes larger being proportional to d^4 and also shows scaling behavior as we addressed in (3.34).

The first law of entanglement entropy. It is widely discussed that in small “ d ” region, there is an interesting relation between the energy and its entanglement entropy of the subsystem [24, 33]. The relation is called the first law of entanglement entropy, which can be understood as an analogy of thermodynamic first law. In short, the relation is given by

$$\Delta E = \mathcal{T} \Delta S, \quad (3.35)$$

where \mathcal{T} is called entanglement temperature, which is inversely proportional to the subsystem size. ΔS means entanglement entropy changes from its background to a new state, where the background is pure AdS space, which corresponds to vacuum defined in (AdS) boundary field theory in holographic dictionary. An interesting property of the entanglement temperature is that it is universal in a sense that it only depends on the shape of the subsystem and the dimensionality of (AdS) boundary spacetime, not any other details of the subsystem.

We find that even in the case that the vector order appears, the universality does not be broken. To discuss this, let us see the energy of the subsystem when we consider wide and thin slabs defined in AdS boundary. In the following discussion, we restrict ourselves

in the case of the subsystem in 4-dimensional spacetime. According to the prescription suggested in [24, 35, 37–41],

$$\Delta E = E - E_g = \int_{\text{subsystem}} d^3x \langle T_{tt} \rangle, \quad (3.36)$$

where $\langle T_{tt} \rangle$ is temporal component of boundary stress-energy tensor, the energy density of the subsystem when the subsystem is excited from its ground state. $\int_{\text{subsystem}} d^3x$ is the spatial volume integration of the subsystem. When, the energy density $\langle T_{tt} \rangle$ is a constant in the subsystem,

$$\Delta E_i = \Sigma_i d \langle T_{tt} \rangle, \quad (3.37)$$

for each slab, where ΔE_1 is the energy for the slab lying on $x_2 - x_3$ plane whereas ΔE_2 is the energy for the slab lying on $x_1 - x_3$ plane. E is the subsystem energy, and E_g is its ground state energy, which corresponds to pure AdS space in its gravity dual. $\langle T_{tt} \rangle$ is related to black brane mass and the relation is

$$\langle T_{tt} \rangle = \frac{3M}{2\kappa_5^2}, \quad (3.38)$$

where M is mass of the 5-dimensional charged black brane near critical point. We read off M from the coefficient of $1/r^4$ term in the metric factor, $N(r)/r^2$ in its large r (small $1/r$) expansion.

In isotropic phase, the mass of the charged black brane, M is given by

$$M^{\text{iso}} = 1 + \frac{32}{3}\alpha^2. \quad (3.39)$$

We note that we rescale the coordinate variables, r , t and x^i in the metric to fix the charged black brane horizon $r_h = 1$.

The first term in (3.39) is related to the energy difference between black brane and pure AdS space. Once we turn on the temporal component of Yang-Mills fields, $B_0^3 = \phi(r)$, the black brane becomes charged and so (electric) chemical potential comes in. This effect comes with α^2 corrections in the spacetime metric, and so in M . In summary, we have

$$\Delta E_i = \Delta_0 E_i + \Delta_\alpha E_i, \quad (3.40)$$

where

$$\Delta_0 E_i = \frac{3}{2\kappa_5^2} \Sigma_i d \quad \text{and} \quad \Delta_\alpha E_i = \frac{16}{\kappa_5^2} \alpha^2 \Sigma_i d. \quad (3.41)$$

We note that $\Delta_0 Q$ represents the difference between the quantity, Q computed in black brane background and in pure AdS background. $\Delta_\alpha Q$ is the α^2 correction to the quantity, Q when the chemical potential is turned on. The entanglement entropy change is given by

$$\Delta S_i = \Delta_0 S + \Delta_\alpha S_i, \quad (3.42)$$

where

$$\Delta_0 S_i = \frac{2}{\kappa_5^2} \Sigma_i \mathcal{A}_i^{(0)} \quad \text{and} \quad \Delta_\alpha S_i = \frac{2}{\kappa_5^2} \alpha^2 \Sigma_i \mathcal{A}_i^{(\alpha)}, \quad (3.43)$$

³In general, $\langle T_{tt} \rangle = \frac{(d-1)M}{2\kappa_{d+1}^2}$, where d is the dimensionality of AdS boundary spacetime [24].

and the surface area $\mathcal{A}_i^{(0)}$ and $\mathcal{A}_i^{(\alpha)}$ are given in (3.15), (3.16), and (3.27). By considering all the details in the above discussion, we get

$$\lim_{d \rightarrow 0} \frac{\Delta E_i}{\Delta S_i} = \lim_{d \rightarrow 0} \frac{\Delta_0 E_i}{\Delta_0 S_i} = \lim_{d \rightarrow 0} \frac{\Delta_\alpha E_i}{\Delta_\alpha S_i} = \mathcal{T}, \quad (3.44)$$

where

$$\mathcal{T} = \frac{80\pi^{5/2}}{\Gamma\left(\frac{1}{3}\right)^3 \Gamma\left(\frac{1}{6}\right)^3 d} \simeq \frac{0.422059}{d} \quad (3.45)$$

In anisotropic phase, $\epsilon^2 \alpha^2$ correction comes into the black brane mass, M by considering backreactions from the vector order, $\omega(r)$. The black brane mass in anisotropic phase is

$$M^{\text{aniso}} = M^{\text{iso}} + \frac{281}{1260} \epsilon^2 \alpha^2, \quad (3.46)$$

which can be read off from the metric factor $N(r)$ as we discussed above. By using black brane temperature (2.19) and (2.21), we obtain

$$\Delta_\epsilon E_i \equiv E_i^{\text{iso}} - E_i^{\text{aniso}} = \frac{843\pi}{34\kappa_5^2} \Sigma_i d T_c \left(1 - \frac{T}{T_c}\right)^\beta, \quad (3.47)$$

with $\beta = 1$. How much entanglement entropy changes when the vector order, $\omega(r)$ is turned on is given in (3.30). Therefore, the ratio of $\Delta_\epsilon E_i$ to $\Delta_\epsilon S_i$ can be computed, which is given by

$$\lim_{d \rightarrow 0} \frac{\Delta_\epsilon E_i}{\Delta_\epsilon S_i} = \frac{80\pi^{5/2}}{\Gamma\left(\frac{1}{3}\right)^3 \Gamma\left(\frac{1}{6}\right)^3 d} = \mathcal{T}, \quad (3.48)$$

where we understand that the entanglement temperature is still universal even in anisotropic phase.

4 Holographic computation of entanglement entropy of a long cylinder with its radius, a and its length, L_1 along x_1 -direction

4.1 Holographic entanglement calculation of cylinder

In this section, we consider a subsystem, of which shape is a cylinder lying along the direction of the vector order, $\omega(r)$ on AdS boundary spacetime (x_1 -direction).⁴ This cylinder is given as, $0 \leq \rho \leq a$, $0 \leq \phi \leq 2\pi$ and $-\frac{L_1}{2} \leq x_1 \leq \frac{L_1}{2}$. The variables, ρ and ϕ are $\rho = \sqrt{x_2^2 + x_3^2}$ and $\phi = \cot^{-1}\left(\frac{x_2}{x_3}\right)$. By using these new coordinate variables, we introduce plane polar coordinate on the $x_2 - x_3$ plane as

$$ds^2 = \frac{1}{z^2} \left\{ -z^2 N(z) \sigma^2(z) dt^2 + \frac{dz^2}{z^2 N(z)} + f^{-4}(z) dx_1^2 + f^2(z) (d\rho^2 + \rho^2 d\phi^2) \right\}, \quad (4.1)$$

⁴We note that there are some of entanglement entropy computations on cylinder. Field theory computations of entanglement entropy by employing numerics are in [35, 36]. For holographic computations, hyperbolic cylinder $R \times H^{d-1}$ is considered [34] and cylinder in the pure AdS background is also considered in [21].

where $z = r^{-1}$, $f(z)$ and $N(z)$ are given in (2.16), (2.17) and (2.18). Now, we consider surface area from the cylinder on AdS boundary, where ϕ and x_1 are to be symmetric directions and we take L_1 is to be very large. The surface area is given by

$$A_1^{cy} = 2\pi L_1 \lim_{\delta \rightarrow 0} \int_{\delta}^{z_*^{cy}} dz z^{-3} \rho(z) \sqrt{\frac{1}{z^2 f^2(z) N(z)} + \left(\frac{d\rho}{dz}\right)^2}, \quad (4.2)$$

where z_*^{cy} is the maximum value of the coordinate z . To minimize the surface, we apply variation principle to the surface. The condition for the extremization is given by

$$\sqrt{\frac{1}{z^2 f^2(z) N(z)} + (\partial_z \rho)^2} = z^3 \frac{\partial}{\partial z} \left(\frac{\rho(z) \partial_z \rho}{z^3 \sqrt{\frac{1}{z^2 f^2(z) N(z)} + (\partial_z \rho)^2}} \right). \quad (4.3)$$

Divergent pieces in the solution, $\rho(z)$. To solve the equation (4.3), we use a fact that the functions $f(z)$ and $N(z)$ have the form of (2.16) together with an expansion with small ε and α such that

$$\rho(r) = \rho_0(z) + \alpha^2 \rho_\alpha(z) + \varepsilon^2 \alpha^2 \rho_\varepsilon(z),$$

up to leading order in $\varepsilon^2 \alpha^2$. The solution can be obtained with a form of series solution in small z , meaning that an expansion near boundary, $z = 0$. The solutions are given by

$$\rho_0 = a - \frac{z^2}{4a} + O(z^4), \quad \rho_\alpha = O(z^4), \quad \text{and} \quad \rho_\varepsilon = O(z^4). \quad (4.4)$$

This solution specifies the divergent pieces of the minimized surface area, which is given by $A_1^{cy} \sim 2\pi L_1 \lim_{\delta \rightarrow 0} \left(\frac{a}{2\delta^2} + \frac{1}{8a} \log \delta \right) + \text{finite}$, where the δ is again the radial cutoff near AdS boundary [21].

In our computation, our purpose is to obtain finite pieces of the entanglement entropy of the cylinder (its minimal area). To do this, we need to impose correct boundary conditions at $z = z_*^{cy}$ as well as $z = \delta$ (on the AdS boundary). However, the solution, (4.4) will require a boundary condition at $z = z_*^{cy}$ as

$$\left. \frac{\partial \rho}{\partial z} \right|_{z=z_*^{cy}} = \infty,$$

since the variable z has a maximum at $z = z_*^{cy}$. This boundary condition is impossible to impose.

The boundary conditions for the inverse solution, $z(\rho)$. Therefore, we may try an inverse solution, $z(\rho)$. To get the solution, we define $z(\rho)$ as a series expansion in ρ ,

$$z(\rho) \equiv z_*^{cy} + \sum_{n=1}^{\infty} b_n \rho^n \quad (4.5)$$

together with boundary conditions

$$1. \quad z(\rho = 0) = z_*^{cy} \quad (\text{automatically satisfied}) \quad (4.6)$$

$$2. \quad z(\rho = a) = z_*^{cy} + \sum_{n=1}^{\infty} b_n a^n = 0, \quad (4.7)$$

where b_n are coefficients of the expansion and z_*^{cy} is the maximum value of the coordinate z .

To find z_*^{cy} , we need to solve a large degree polynomial equation (4.7) (practically n-degree by truncation), which is given by

$$z_*^{cy} = - \sum_{n=1}^{\infty} a^n b_n. \tag{4.8}$$

The final boundary condition at the turning point ($z = z_*^{cy}$) is $\left. \frac{dz(\rho)}{d\rho} \right|_{\rho=0} = 0$ being given by

$$3. \quad \left. \frac{dz(\rho)}{d\rho} \right|_{\rho=0} = \sum_{n=1}^{\infty} n b_n \rho^{n-1} \Big|_{\rho=0} = 0, \tag{4.9}$$

and that requires $b_1 = 0$. Therefore, the form of the solution is

$$z(\rho) = z_*^{cy} + \sum_{n=2}^{\infty} b_n \rho^n. \tag{4.10}$$

The solution, $z(\rho)$ will have the following terms in it:

$$z(\rho) = z_0(\rho) + \alpha^2 z^{(\alpha)}(\rho) + \varepsilon^2 \alpha^2 z^{(\varepsilon)}(\rho), \tag{4.11}$$

where z_0 is the solution in the background of black brane, and $z^{(\alpha)}$ is α^2 correction and finally $z^{(\varepsilon)}$ is the $\varepsilon^2 \alpha^2$ correction near the critical point, $T = T_c$. Each $z_0(\rho)$, $z^{(\alpha)}(\rho)$, and $z^{(\varepsilon)}(\rho)$ is a series solution in ρ and so satisfies the same boundary conditions (4.6), (4.7) and (4.9) as we have discussed above. We note that we define the maximum value of each solution as $z_0(0) = z_*$, $z^{(\alpha)}(0) = z_*^\alpha$ and $z^{(\varepsilon)}(0) = z_*^\varepsilon$ and so

$$z_*^{cy} = z_* + \alpha^2 z_*^\alpha + \varepsilon^2 \alpha^2 z_*^\varepsilon. \tag{4.12}$$

Getting solutions. Now, we illustrate the procedure how to get the solutions.

- We substitute the trial solution (4.11) into equation (4.3) and get series solutions for z_0 , $z^{(\alpha)}$, and $z^{(\varepsilon)}$, which are given in appendix B.1 in detail. We obtain each series solution upto $O(\rho^{30})$. First, by applying the boundary condition (4.7) to $z_0(\rho)$ solution, we get the ratio of a to z_* , i.e. $\frac{a}{z_*}$, with a given z_* . By using this information, we can get the value of a with the given z_* . We summarize some of the results in table 1.
- We also solve equations for $z^{(\alpha)}(\rho)$ and $z^{(\varepsilon)}(\rho)$. The equations and the solutions are given in appendix B.1. With the given values of a that we obtained from $z_0(\rho)$ solution, we compute how much the turning point, z_*^{cy} (maximum value of z) changes by α^2 and $\varepsilon^2 \alpha^2$ corrections by employing the solutions of $z^{(\alpha)}(\rho)$ and $z^{(\varepsilon)}(\rho)$. These values are also given in table 1.

| | | | | | | |
|-----------------------------|----------|----------------------|----------------------|----------------------|----------------------|----------------------|
| z_* | 0 | 0.05 | 0.10 | 0.15 | 0.20 | 0.25 |
| a | 0 | 0.0398102 | 0.0796221 | 0.119444 | 0.159297 | 0.199223 |
| a/z_* deg:38 | 0.796204 | 0.796205 | 0.796221 | 0.796293 | 0.796485 | 0.796891 |
| z_*^α deg:30 | 0 | $-7.34078 * 10^{-7}$ | $-2.33482 * 10^{-5}$ | $-1.75502 * 10^{-4}$ | $-7.28959 * 10^{-4}$ | $-2.18304 * 10^{-3}$ |
| z_*^ε deg:30 | 0 | $-1.52560 * 10^{-8}$ | $-4.76626 * 10^{-7}$ | $-3.47876 * 10^{-6}$ | $-1.38778 * 10^{-5}$ | $-3.95175 * 10^{-5}$ |

| | | | | | | |
|-----------------------------|----------------------|----------------------|----------------------|----------------------|----------------------|--|
| z_* | 0.30 | 0.35 | 0.40 | 0.45 | 0.50 | |
| a | 0.239290 | 0.279601 | 0.320305 | 0.361608 | 0.403790 | |
| a/z_* deg:38 | 0.797632 | 0.798860 | 0.800763 | 0.803573 | 0.807580 | |
| z_*^α deg:30 | $-5.30576 * 10^{-3}$ | $-1.11452 * 10^{-2}$ | $-2.10030 * 10^{-2}$ | $-3.63615 * 10^{-2}$ | $-5.87538 * 10^{-2}$ | |
| z_*^ε deg:30 | $-9.05120 * 10^{-5}$ | $-1.77833 * 10^{-4}$ | $-3.11644 * 10^{-4}$ | $-4.99873 * 10^{-4}$ | $-7.47390 * 10^{-4}$ | |

Table 1. In this table, we list the values of a (the radius of the cylinder), z_*^α (the α^2 correction to the maximum value of z_*), and z_*^ε (the $\varepsilon^2\alpha^2$ correction to the maximum value of z_*) with given values of z_* . These values are obtained by solving boundary condition (4.7). Solutions are obtained upto $O(a^{38})$ for z_0 solution and upto $O(a^{30})$ for $z^{(\alpha)}$ and $z^{(\varepsilon)}$ solutions.

4.2 Evaluation of surface area and subtraction of UV-divergence

In this subsection, we plug the solutions (4.11) into the surface area (4.2) to evaluate it(The detailed forms of the solutions are given in (B.3), (B.6) and (B.10)). We notice that once one expands the minimal area by plugging the solution (4.11), the divergent pieces of the area will appear. These need to be subtracted. As we did for the case of slabs, we subtract the pure AdS parts from the surface area as follows.

Once we evaluate the surface area by employing small α and ε expansion upto leading order α^2 and $\varepsilon^2\alpha^2$, then we have

$$A_1^{cy} \equiv 2\pi L_1 \left(\gamma^{(0)} + \alpha^2 \gamma^{(\alpha)} + \varepsilon^2 \alpha^2 \gamma^{(\varepsilon)} \right),$$

where the divergence pieces are given in $\gamma^{(0)}$ only. When $\alpha = 0$ and $\varepsilon = 0$, A_1^{cy} becomes $2\pi L_1 \gamma^{(0)}$. $\gamma^{(0)}$ is the surface area in the background of black brane geometry, when $f(z) = \sigma(z) = 1$ and $z^2 N(z) = 1 - z^4$. In the factor of $z^2 N(z) = 1 - z^4$, the second terms in $z^2 N(z)$ is the effect of black brane mass. Therefore once we consider a new factor,

$$z^2 N(z, \xi) \equiv 1 - \xi z^4. \quad (4.13)$$

We consider such a new metric factor $z^2 N(z, \xi)$ and get $\gamma^{(0)}$ again. Then if $\xi = 0$, the solution is in the background of pure AdS, and if $\xi = 1$ it becomes in the background of black brane.

To regularize the surface area $\gamma^{(0)}$, we get solutions of z_0 again by employing power expansion order by order in ξ . This means that we try the following form of the solutions,

$$z_0 = z_0^A + \xi z_0^B + O(\xi^2), \quad (4.14)$$

together with the new metric factor, $N(z, \xi)$. The analytic forms of the solutions for z_0^A and z_0^B are given in appendix B.2. Then, we get the surface area $\gamma^{(0)}$ in power expansion in ξ , as a form of

$$\gamma^{(0)} = \gamma^{(AdS)} + \xi\gamma^{(\xi)} + O(\xi^2), \quad (4.15)$$

where $\gamma^{(AdS)}$ contains the divergence pieces, which needs to be subtracted. We take the first order in ξ only to estimate the regularized part, and this becomes more accurate near boundary calculation since $z \ll 1$ there. Finally we take $\xi = 1$. Then, we define $A_1^{cy(\text{ren})}$ as

$$A_1^{cy(\text{ren})} \equiv A_1^{cy} - A_1^{cy(AdS)}, \quad (4.16)$$

where $A_1^{cy(AdS)} \equiv 2\pi L_1 \gamma^{(AdS)}$. Therefore,

$$A_1^{cy(\text{ren})} \equiv 2\pi L_1 \left(\gamma^{(\xi)} + \alpha^2 \gamma^{(\alpha)} + \varepsilon^2 \alpha^2 \gamma^{(\varepsilon)} \right),$$

and our renormalized entanglement entropy $S^{cy(\text{ren})}$ for the cylinder is given by

$$S_{cy}^{(\text{ren})} = \frac{2\pi}{\kappa_5^2} A_1^{cy(\text{ren})}. \quad (4.17)$$

Entanglement entropy of Cylinder. $\gamma^{(\xi)}$, $\gamma^{(\alpha)}$ and $\gamma^{(\varepsilon)}$ are graphically obtained in figure. 1, 2 and 3 in order. The analytic forms of these are given in appendix B.3. Their leading behaviors when a is small are given by

$$\gamma^{(\xi)}(a) = 0.73228506a^3 + O(a^4), \quad (4.18)$$

$$\gamma^{(\alpha)}(a) = 7.8111218a^3 + O(a^4), \quad (4.19)$$

$$\gamma^{(\varepsilon)}(a) = 0.1633128a^3 + O(a^4). \quad (4.20)$$

Once we define $\Delta_\varepsilon S_{cy} = S_{cy}^{\text{iso}} - S_{cy}^{\text{aniso}}$ as we discussed in the slab case, we find that

$$\Delta_\varepsilon S_{cy} = \frac{5040\pi^2 L_1}{17\kappa_5^2} \gamma^{(\varepsilon)}(a) T_c \left(1 - \frac{T}{T_c} \right)^\beta, \quad (4.21)$$

where a and L_1 is the radius and the length of the cylinder. Our analytic computation shows that holographic entanglement entropy excess $\Delta_\varepsilon S_{cy}$ for cylinder also presents scaling behavior $\sim \left(1 - \frac{T}{T_c} \right)^\beta$ and its critical exponent $\beta = 1$.

The first law of entanglement entropy and entanglement temperature. In figure. 4, we plot the following quantities in order:

$$\frac{1}{a} \frac{\Delta_0 S_{cy}}{\Delta_0 E} = \frac{8\pi\gamma^{(\xi)}(a)}{3a^3} \quad (\xi - \text{graph}), \quad (4.22)$$

$$\frac{1}{a} \frac{\Delta_\alpha S_{cy}}{\Delta_\alpha E} = \frac{\pi\gamma^{(\alpha)}(a)}{4a^3} \quad (\alpha^2 - \text{graph}), \quad (4.23)$$

$$\frac{1}{a} \frac{\Delta_\varepsilon S_{cy}}{\Delta_\varepsilon E} = \frac{3360\pi\gamma^{(\varepsilon)}(a)}{281a^3} \quad (\varepsilon^2\alpha^2 - \text{graph}), \quad (4.24)$$

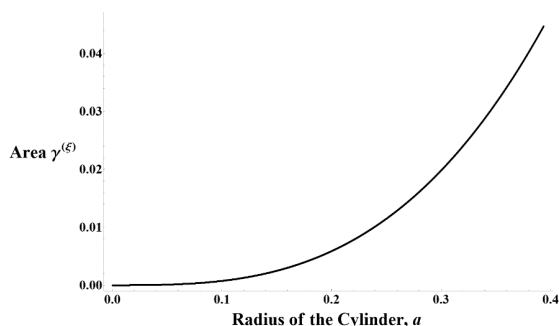


Figure 1. $\gamma^{(\epsilon)}(a) = 0.73228506a^3 + \dots$, from $a = 7.87386 \times 10^{-5}$ to $a = 0.393693$, 5000 data points.

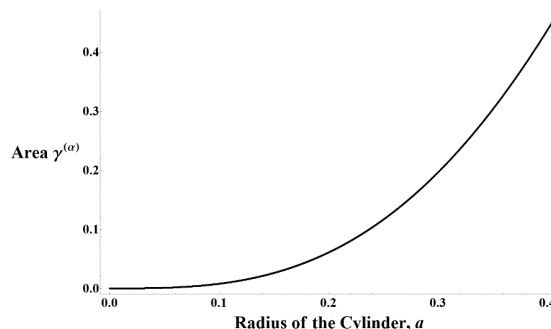


Figure 2. $\gamma^{(\alpha)}(a) = 7.8111218a^3 + \dots$, from $a = 7.96204 \times 10^{-5}$ to $a = 0.403790$, 5000 data points.

and it turns out that as a approach zero, they meet at one point. We again note that $\Delta_0 Q$ represents the difference between the quantity, Q computed in black brane background and in pure AdS background. $\Delta_\alpha Q$ is the α^2 correction to the quantity, Q when the chemical potential is turned on. Finally, Δ_ϵ is $\epsilon^2 \alpha^2$ correction to the quantity, Q when the vector order appears near the critical point. Therefore, we conclude that when $a \rightarrow 0$,

$$\lim_{a \rightarrow 0} \frac{1}{a} \frac{\Delta S_{cy}}{\Delta E} = \lim_{a \rightarrow 0} \frac{1}{a} \frac{\Delta_0 S_{cy}}{\Delta_0 E} = \lim_{a \rightarrow 0} \frac{1}{a} \frac{\Delta_\alpha S_{cy}}{\Delta_\alpha E} = \lim_{a \rightarrow 0} \frac{1}{a} \frac{\Delta_\epsilon S_{cy}}{\Delta_\epsilon E} = c_{\text{ent}}^{-1}, \quad (4.25)$$

where

$$c_{\text{ent}} = 0.163004 \pm 0.000001. \quad (4.26)$$

This value is obtained by computing the average and standard deviation of the values of the functions (4.22), (4.23), and (4.24) at $a = 0$. By using the definition of entanglement temperature (3.44), we understand that even in the case that the vector order appears in anisotropic phase, the first law of entanglement entropy is retained. The entanglement temperature is given by

$$\mathcal{T}_{cy} = \frac{c_{\text{ent}}}{a}. \quad (4.27)$$

5 Discussion

In this paper, we explore 4-dimensional holographic anisotropic super fluids defined on the boundary of 5-dimensional asymptotically AdS spacetime near its critical point $T = T_c$, where a vector order parameter appears, and it breaks SO(3)-rotational symmetry of spacetime down to SO(2). The gravity dual of such a system is Einstein-SU(2)Yang-Mills theory, defined in asymptotically AdS spacetime. To understand properties of this system, we compute holographic entanglement entropy in the background of the charged black brane solution of this gravity system. We apply an analytic method and obtain holographic entanglement entropies of subsystems with shapes of wide and thin slabs and a long cylinder.

For the wide and thin slabs, we consider two different spatial directions: one is lying along a direction which is parallel to the vector order whereas another is perpendicular to

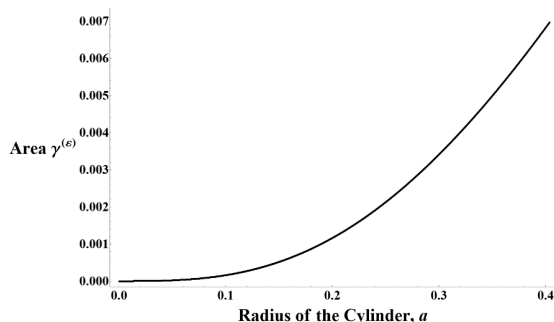


Figure 3. $\gamma^{(\epsilon)}(a) = 0.1633128a^3 + \dots$, from $a = 7.96204 \times 10^{-5}$ to $a = 0.403790$, 5000 data points.

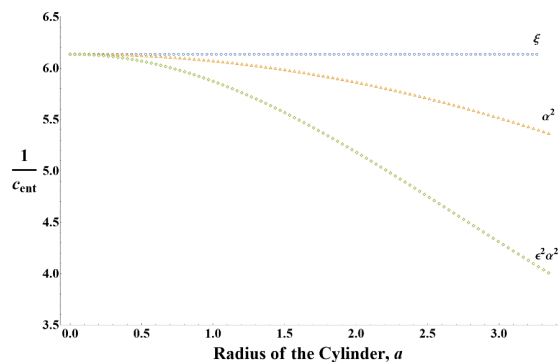


Figure 4. $\xi \rightarrow \lim_{a \rightarrow 0} \frac{8\pi\gamma^{(\epsilon)}(a)}{3a^3} = 6.134777049077025$,
 $a^2 \rightarrow \lim_{a \rightarrow 0} \frac{\pi\gamma^{(\alpha)}(a)}{4a^3} = 6.134840767351422$,
 $\epsilon^2 a^2 \rightarrow \lim_{a \rightarrow 0} \frac{3360\pi\gamma^{(\epsilon)}(a)}{281a^3} = 6.134840676290574$,
 100 data points each

the vector order. For the cylinder case, we consider the cylinder lying along the vector order only. The entanglement entropies that we obtained for the slab and cylinder cases share universal properties: these show a scaling behavior near critical point, which has a form of

$$\Delta_\epsilon S \sim \left(1 - \frac{T}{T_c}\right)^\beta, \quad (5.1)$$

where $\Delta_\epsilon S = S^{\text{iso}} - S^{\text{aniso}}$, and S^{iso} is the entanglement entropy in isotropic phase whereas S^{aniso} is that in anisotropic phase. The critical exponent, $\beta = 1$ for all of the cases that we examine. Therefore, we understand that the critical exponent $\beta = 1$ is probably the common feature of the entanglement entropy near the critical point of the system. We note that the analytic approach is valid when $\alpha = \frac{\kappa_5}{g}$ is small, and in this case, the system undergoes second order phase transition near the critical point. We restrict our analysis in this case only.

However, an interesting feature occurs when we consider anisotropy. The entanglement entropy of slabs has the following expansion near the critical point

$$\Delta_\epsilon S_i = C_i(d) \left(1 - \frac{T}{T_c}\right)^\beta, \quad (5.2)$$

where $i = 1, 2$ and $i = 1$ is for the slab being parallel to the vector order whereas $i = 2$ is for the slab being perpendicular to the vector order. We assume that the shapes of those two slabs are the same but their directions are different. We determine the coefficient, $C_i(d)$, by employing small “ d ” expansion such as

$$C_i(d) = C_i^{(2)} d^2 + C_i^{(4)} d^4 + \dots \quad (5.3)$$

where the d is the thickness of the slabs. In the small d region, we probe ultraviolet degrees of freedom and it corresponds to that the extended minimal surface to the bulk from the

slab is still probing the bulk region near the AdS boundary. However, condensation is an infrared effect. This means that we need to probe deeper in the infrared region to see the effects of condensation. In its holographic dual, as d grows, the extended minimal surface to the bulk from the slab probes deeper in the bulk.

In the small d region, the term being proportional to $C^{(2)}$ is the most dominant and it turns out that $C_1^{(2)} = C_2^{(2)}$. This implies that the ultraviolet degrees of freedom is still universal in a sense that they are independent of the directions of the vector order parameter. An interesting anisotropy appears in $C_i^{(4)}$ such that $C_1^{(4)} \neq C_2^{(4)}$. This observation leads us to define a new order parameter from entanglement entropy, which is defined as

$$\mathcal{O}_{12} \equiv S_1 - S_2. \tag{5.4}$$

We understand that $O_{12} = 0$ above the critical temperature since SO(3)-rotational symmetry is retained. However, O_{12} shows critical behavior together with its non-zero coefficient near the critical point and it can be an indication of phase transition.

With the same reason, the condensation does not spoil the first law of entanglement entropy, since the law holds in the $d \rightarrow 0$ limit, which implies that it is ultraviolet physics. In the small size limit of the subsystem ($d \rightarrow 0$ limit), it turns out that the ratio of entropy change to total energy change of the subsystem is universal. The term being proportional to $C^{(4)}$ is relatively infrared effect and it is subleading in small d expansion.

In conclusion, in anisotropic holographic superfluid system, we find that the system presents universal properties and anisotropy at the same time. The universal properties are scaling behaviors of the entanglement entropies and all of the subsystems that we study share their critical exponent $\beta = 1$. When one looks at ultraviolet degrees of freedom, the first law of entanglement entropy is held for all the subsystems that we look at. This is also a universal feature in a sense that it does not depend on the direction of the vector order parameter. However, if one averts one's eyes to the infrared region, one can see a fact that entanglement entropy depends on the direction of the order parameter. By using this fact, one can define an interesting order parameter near the critical point.

Acknowledgments

J.H.O thanks his W.J. and Y.J. This work was supported by the National Research Foundation of Korea(NRF) grant funded by the Korea government (MSIT) (No. 2021R1F1A1047930). CP was supported by the National Research Foundation of Korea (NRF) grant funded by the Korea government (MSIT) (No. NRF-2019R1A2C1006639).

A Slabs on the x_2 - x_3 and x_3 - x_1 planes

For the computations of the slabs, we need to evaluate the following form of the integration:

$$I_n \equiv \int_1^\infty \frac{u^n}{\sqrt{u^6 - 1}} du, \tag{A.1}$$

where n is an integer. For some specific n , there are some results:

$$I_{-8} = \frac{4\sqrt{\pi}\Gamma\left(\frac{2}{3}\right)}{7\Gamma\left(\frac{1}{6}\right)}, \quad I_{-6} = \frac{\sqrt{\pi}\Gamma\left(\frac{1}{3}\right)}{15\Gamma\left(\frac{5}{6}\right)}, \quad I_{-4} = \frac{1}{3}, \quad I_{-2} = \frac{\sqrt{\pi}\Gamma\left(\frac{2}{3}\right)}{\Gamma\left(\frac{1}{6}\right)}, \quad I_0 = \frac{\sqrt{\pi}\Gamma\left(\frac{1}{3}\right)}{6\Gamma\left(\frac{5}{6}\right)},$$

$$I_4 = \lim_{\delta \rightarrow 0} \left[\frac{1}{2\delta^2} + O(\delta^3) \right] - \frac{\sqrt{\pi}\Gamma\left(\frac{2}{3}\right)}{2\Gamma\left(\frac{1}{6}\right)}$$

We define variables $s = 1/r_*$ and $u = rs$. In fact, to get the area of the slabs analytically, we expand the metric factors appearing in the calculation in terms of s , where we expand $f(r)$ and $N(r)$ in terms of s . They are given by

$$f = 1 - \frac{1}{18} \frac{(1-2r^2)}{(1+r^2)^4} \varepsilon^2 \alpha^2 \tag{A.2}$$

$$= 1 - \frac{1}{18} \varepsilon^2 \alpha^2 \left(1 - \frac{2u^2}{s^2}\right) \left(1 + \frac{u^2}{s^2}\right)^{-4}$$

$$= 1 + \frac{\varepsilon^2 \alpha^2}{9u^6} s^6 - \frac{\varepsilon^2 \alpha^2}{2u^8} s^8 + O(s^9)$$

and

$$N = r^2 - \frac{1}{r^2} + \frac{32}{3} \alpha^2 \left(\frac{1}{r^4} - \frac{1}{r^2}\right) - \frac{4\varepsilon^2 \alpha^2}{9r^2} \left[\frac{281}{560} \left(1 - \frac{1}{r^2}\right) - \frac{3r^2}{2(1+r^2)^2} + \frac{1+2r^2}{r^2(1+r^2)^3} \right]$$

$$= r^2 \left(1 - \frac{1}{r^4}\right) \left[1 - \frac{32}{3} \alpha^2 r^{-2} (1+r^2)^{-1} + \frac{\varepsilon^2 \alpha^2}{1260} (279r^{-2} + 837 - 3r^2 - 281r^4) (1+r^2)^{-4} \right]$$

$$= \frac{u^2}{s^2} \left[1 - \left(1 + \frac{32}{3} \alpha^2 + \frac{281}{1260} \varepsilon^2 \alpha^2\right) \frac{s^4}{u^4} + \left(\frac{32}{3} \alpha^2 + \frac{1121}{1260} \varepsilon^2 \alpha^2\right) \frac{s^6}{u^6} - \frac{4\varepsilon^2 \alpha^2}{3} \frac{s^8}{u^8} \right. \\ \left. + \frac{10\varepsilon^2 \alpha^2}{9} \frac{s^{10}}{u^{10}} \right] + O(s^9) \tag{A.3}$$

A.1 Slab on AdS boundary and divergence subtraction

For surface area computation in AdS space, we use metric (2.7) but the metric factors of f , σ , and N are replaced by

$$\sigma = 1, \quad f = 1, \quad N(r) = r^2.$$

Then, the relations between d , s , and the surface area $A_1^{(AdS)}$ are given by

$$d = 2 \int_{r_*}^{\infty} \frac{dr}{\sqrt{\frac{r^2 N(r)}{f^4} \left(\frac{r^6}{r_*^6} - 1\right)}} = 2 \int_{r_*}^{\infty} \frac{dr}{r^2 \sqrt{\frac{r^6}{r_*^6} - 1}} = \frac{2\sqrt{\pi}\Gamma\left(\frac{2}{3}\right)}{\Gamma\left(\frac{1}{6}\right)} s,$$

namely,

$$s(d) = \frac{\Gamma\left(\frac{1}{6}\right)}{2\sqrt{\pi}\Gamma\left(\frac{2}{3}\right)} d.$$

The surface area $A_1^{(AdS)}$ is given by

$$\begin{aligned}
 A_1^{(AdS)} &= 2L_2L_3 \int_{r_*}^{\infty} dr \frac{r^2 f^2}{\sqrt{N(r)}} \left(1 - \frac{r_*^6}{r^6}\right)^{-\frac{1}{2}} = 2\Sigma_1 \int_{r_*}^{\infty} dr \frac{r}{\sqrt{1 - \frac{r_*^6}{r^6}}} \\
 &= \lim_{\delta \rightarrow 0} \frac{1}{\delta^2} - \frac{\sqrt{\pi} \Gamma\left(\frac{2}{3}\right)}{\Gamma\left(\frac{1}{6}\right)} \frac{1}{s^2} \\
 &= \lim_{\delta \rightarrow 0} \frac{1}{\delta^2} + C_{23}^{-2} \frac{1}{d^2}.
 \end{aligned}$$

Finally, we get

$$\frac{A_1^{(\text{ren})}}{\Sigma_1} \equiv \frac{A_1 - A_1^{(AdS)}}{\Sigma_1} = C_{23}^2 d^2 + C_{23}^4 d^4 + C_{23}^6 d^6 + O(d^7). \quad (\text{A.4})$$

A.2 Slab on the x_2 - x_3 plane

The relation between the thickness of the slab “ d ” and r_* , maximal depth of the stretched surface (or, turning point) for the slab on the x_2 - x_3 plane is given by

$$\begin{aligned}
 d &= 2 \int_{r_*}^{\infty} \frac{dr}{\sqrt{\frac{r^2 N(r)}{f^4(r)} \left(\frac{r^6}{r_*^6} - 1\right)}} = \int_1^{\infty} du \frac{2}{u \sqrt{u^6 - 1}} \frac{f^2(u/s)}{\sqrt{N(u/s)}} \quad (\text{A.5}) \\
 &= \int_1^{\infty} du \frac{2}{u \sqrt{u^6 - 1}} \left(1 + \frac{2\varepsilon^2 \alpha^2}{9u^6} s^6 - \frac{\varepsilon^2 \alpha^2}{u^8} s^8\right) \frac{s}{u} \left[1 + \frac{1}{2} \left(1 + \frac{32}{3} \alpha^2 + \frac{281}{1260} \varepsilon^2 \alpha^2\right) \frac{s^4}{u^4}\right. \\
 &\quad \left. - \frac{1}{2} \left(\frac{32}{3} \alpha^2 + \frac{1121}{1260} \varepsilon^2 \alpha^2\right) \frac{s^6}{u^6} + \frac{2\varepsilon^2 \alpha^2}{3} \frac{s^8}{u^8}\right] \\
 &= (2I_{-2}) s + I_{-6} \left(1 + \frac{32}{3} \alpha^2 + \frac{281}{1260} \varepsilon^2 \alpha^2\right) s^5 - I_{-8} \left(\frac{32}{3} \alpha^2 + \frac{187}{420} \varepsilon^2 \alpha^2\right) s^7 + O(s^8) \\
 &= \frac{2\sqrt{\pi} \Gamma\left(\frac{2}{3}\right)}{\Gamma\left(\frac{1}{6}\right)} s + \frac{\sqrt{\pi} \Gamma\left(\frac{1}{3}\right)}{15\Gamma\left(\frac{5}{6}\right)} \left(1 + \frac{32}{3} \alpha^2 + \frac{281}{1260} \varepsilon^2 \alpha^2\right) s^5 - \frac{4\sqrt{\pi} \Gamma\left(\frac{2}{3}\right)}{7\Gamma\left(\frac{1}{6}\right)} \left(\frac{32}{3} \alpha^2 + \frac{187}{420} \varepsilon^2 \alpha^2\right) s^7 \\
 &\quad + O(s^8),
 \end{aligned}$$

where we expand the integration in terms of s upto its 7th order.

From this form of the expansion, the expression for s can be given in series of small d .

$$\begin{aligned}
 s(d) &= \frac{\Gamma\left(\frac{1}{6}\right)}{2\sqrt{\pi} \Gamma\left(\frac{2}{3}\right)} d - \frac{5\Gamma\left(\frac{1}{3}\right) \Gamma\left(\frac{1}{6}\right)^6}{6912\sqrt{\pi^5} \Gamma\left(\frac{2}{3}\right)^6 \Gamma\left(\frac{5}{6}\right)} \left(1 + \frac{32}{3} \alpha^2 + \frac{281}{1260} \varepsilon^2 \alpha^2\right) d^5 \quad (\text{A.6}) \\
 &\quad + \frac{\Gamma\left(\frac{1}{6}\right)^7}{448\sqrt{\pi^7} \Gamma\left(\frac{2}{3}\right)^7} \left(\frac{32}{3} \alpha^2 + \frac{187}{420} \varepsilon^2 \alpha^2\right) d^7 + O(d^8)
 \end{aligned}$$

A_1 in terms of s , upto 6th order is given by.

$$\begin{aligned}
 \frac{A_1}{L_2 L_3} &= 2 \int_{r_*}^{\infty} dr \frac{r^2 f^2(r)}{\sqrt{N(r)}} \left(1 - \frac{r^6}{r_*^6}\right)^{-\frac{1}{2}} \\
 &= \int_1^{\infty} du \frac{2u^5}{\sqrt{u^6 - 1}} \frac{1}{s^3} \frac{f^2(u/s)}{\sqrt{N(u/s)}} \\
 &= 2I_4 \frac{1}{s^2} + I_0 \left(1 + \frac{32}{3}\alpha^2 + \frac{281}{1260}\varepsilon^2\alpha^2\right) s^2 - I_{-2} \left(\frac{32}{3}\alpha^2 + \frac{187}{420}\varepsilon^2\alpha^2\right) s^4 \\
 &\quad + I_{-4} \left(\frac{3}{4} + 16\alpha^2 - \frac{93}{280}\varepsilon^2\alpha^2\right) s^6 + O(s^7) \\
 &= \lim_{\delta \rightarrow 0} \frac{1}{\delta^2} - \frac{\sqrt{\pi}\Gamma\left(\frac{2}{3}\right)}{\Gamma\left(\frac{1}{6}\right)} \frac{1}{s^2} + \frac{\sqrt{\pi}\Gamma\left(\frac{1}{3}\right)}{6\Gamma\left(\frac{5}{6}\right)} \left(1 + \frac{32}{3}\alpha^2 + \frac{281}{1260}\varepsilon^2\alpha^2\right) s^2 \\
 &\quad - \frac{\sqrt{\pi}\Gamma\left(\frac{2}{3}\right)}{\Gamma\left(\frac{1}{6}\right)} \left(\frac{32}{3}\alpha^2 + \frac{187}{420}\varepsilon^2\alpha^2\right) s^4 + \left(\frac{1}{4} + \frac{16}{3}\alpha^2 - \frac{31}{280}\varepsilon^2\alpha^2\right) s^6 + O(s^7)
 \end{aligned} \tag{A.7}$$

Finally, by using the relations (A.6) and (A.7), we get

$$\frac{A_1}{L_2 L_3} = \lim_{\delta \rightarrow 0} \frac{1}{\delta^2} + C_{23}^{-2} \frac{1}{d^2} + C_{23}^2 d^2 + C_{23}^4 d^4 + C_{23}^6 d^6 + O(d^7) \tag{A.8}$$

where

$$\begin{aligned}
 C_{23}^{-2} &= -\frac{32\sqrt{\pi^9}}{3\sqrt{3}} \frac{1}{\Gamma\left(\frac{1}{3}\right)^3 \Gamma\left(\frac{1}{6}\right)^3} \\
 C_{23}^2 &= \frac{3}{320\sqrt{\pi^7}} \Gamma\left(\frac{1}{3}\right)^3 \Gamma\left(\frac{1}{6}\right)^3 \left(1 + \frac{32}{3}\alpha^2 + \frac{281}{1260}\varepsilon^2\alpha^2\right) \\
 C_{23}^4 &= -\frac{3\sqrt{3}}{28\sqrt{\pi^9}} \Gamma\left(\frac{1}{3}\right)^3 \Gamma\left(\frac{1}{6}\right)^3 \left(\alpha^2 + \frac{187}{4480}\varepsilon^2\alpha^2\right) \\
 C_{23}^6 &= \frac{27}{16384\pi^9} \Gamma\left(\frac{1}{3}\right)^6 \Gamma\left(\frac{1}{6}\right)^6 \left(1 - \frac{13\sqrt{3}}{1800\pi^{5/2}} \Gamma\left(\frac{1}{3}\right)^3 \Gamma\left(\frac{1}{6}\right)^3\right) \\
 &\quad + \frac{9}{256\pi^9} \Gamma\left(\frac{1}{3}\right)^6 \Gamma\left(\frac{1}{6}\right)^6 \left(1 - \frac{13\sqrt{3}}{1800\pi^{5/2}} \Gamma\left(\frac{1}{3}\right)^3 \Gamma\left(\frac{1}{6}\right)^3\right) \alpha^2 \\
 &\quad - \frac{837}{1146880\pi^9} \Gamma\left(\frac{1}{3}\right)^6 \Gamma\left(\frac{1}{6}\right)^6 \left(1 + \frac{3653\sqrt{3}}{502200\pi^{5/2}} \Gamma\left(\frac{1}{3}\right)^3 \Gamma\left(\frac{1}{6}\right)^3\right) \varepsilon^2\alpha^2,
 \end{aligned}$$

with $\Gamma\left(\frac{2}{3}\right)$ and $\Gamma\left(\frac{5}{6}\right)$, which are

$$\begin{aligned}
 \Gamma\left(\frac{2}{3}\right) &= \frac{2\pi}{\sqrt{3}\Gamma\left(\frac{1}{3}\right)}, \\
 \Gamma\left(\frac{5}{6}\right) &= \frac{2\pi}{\Gamma\left(\frac{1}{6}\right)}.
 \end{aligned}$$

A.3 Slab on the x_3 - x_1 plane

In this subsection we find the expression of A_2 in terms of d , following the same steps as we did in A.1. First, d is expanded in terms of s upto its 7th order.

$$\begin{aligned}
 d &= 2 \int_{r_*}^{\infty} \frac{dr}{\sqrt{r^2 f^2(r) N(r) \left(\frac{r^6}{r_*^6} - 1\right)}} = \int_1^{\infty} du \frac{2}{u\sqrt{u^6-1}} \frac{1}{f(u/s)\sqrt{N(u/s)}} \quad (\text{A.9}) \\
 &= \int_1^{\infty} du \frac{2}{u\sqrt{u^6-1}} \left(1 - \frac{\varepsilon^2 \alpha^2}{9u^6} s^6 + \frac{\varepsilon^2 \alpha^2}{2u^8} s^8\right) \frac{s}{u} \left[1 + \frac{1}{2} \left(1 + \frac{32}{3} \alpha^2 + \frac{281}{1260} \varepsilon^2 \alpha^2\right) \frac{s^4}{u^4}\right. \\
 &\quad \left. - \frac{1}{2} \left(\frac{32}{3} \alpha^2 + \frac{1121}{1260} \varepsilon^2 \alpha^2\right) \frac{s^6}{u^6} + \frac{2\varepsilon^2 \alpha^2}{3} \frac{s^8}{u^8}\right] \\
 &= (2I_{-2}) s + I_{-6} \left(1 + \frac{32}{3} \alpha^2 + \frac{281}{1260} \varepsilon^2 \alpha^2\right) s^5 - I_{-8} \left(\frac{32}{3} \alpha^2 + \frac{467}{420} \varepsilon^2 \alpha^2\right) s^7 + O(s^8) \\
 &= \frac{2\sqrt{\pi} \Gamma\left(\frac{2}{3}\right)}{\Gamma\left(\frac{1}{6}\right)} s + \frac{\sqrt{\pi} \Gamma\left(\frac{1}{3}\right)}{15\Gamma\left(\frac{5}{6}\right)} \left(1 + \frac{32}{3} \alpha^2 + \frac{281}{1260} \varepsilon^2 \alpha^2\right) s^5 - \frac{4\sqrt{\pi} \Gamma\left(\frac{2}{3}\right)}{7\Gamma\left(\frac{1}{6}\right)} \left(\frac{32}{3} \alpha^2 + \frac{467}{420} \varepsilon^2 \alpha^2\right) s^7 \\
 &\quad + O(s^8)
 \end{aligned}$$

The expression for s is given in series of small d .

$$\begin{aligned}
 s(d) &= \frac{\Gamma\left(\frac{1}{6}\right)}{2\sqrt{\pi} \Gamma\left(\frac{2}{3}\right)} d - \frac{5\Gamma\left(\frac{1}{3}\right) \Gamma\left(\frac{1}{6}\right)^6}{6912\sqrt{\pi^5} \Gamma\left(\frac{2}{3}\right)^6 \Gamma\left(\frac{5}{6}\right)} \left(1 + \frac{32}{3} \alpha^2 + \frac{281}{1260} \varepsilon^2 \alpha^2\right) d^5 \quad (\text{A.10}) \\
 &\quad + \frac{\Gamma\left(\frac{1}{6}\right)^7}{448\sqrt{\pi^7} \Gamma\left(\frac{2}{3}\right)^7} \left(\frac{32}{3} \alpha^2 + \frac{467}{420} \varepsilon^2 \alpha^2\right) d^7 + O(d^8)
 \end{aligned}$$

A_2 in terms of s upto 6th order is given by

$$\begin{aligned}
 \frac{A_2}{L_3 L_1} &= 2 \int_{r_*}^{\infty} dr \frac{r^2}{f(r)\sqrt{N(r)}} \left(1 - \frac{r^6}{r_*^6}\right)^{-\frac{1}{2}} \quad (\text{A.11}) \\
 &= \int_1^{\infty} du \frac{2u^5}{\sqrt{u^6-1}} \frac{1}{s^3 f(u/s)\sqrt{N(u/s)}} \\
 &= 2I_4 \frac{1}{s^2} + I_0 \left(1 + \frac{32}{3} \alpha^2 + \frac{281}{1260} \varepsilon^2 \alpha^2\right) s^2 - I_{-2} \left(\frac{32}{3} \alpha^2 + \frac{467}{420} \varepsilon^2 \alpha^2\right) s^4 \\
 &\quad + I_{-4} \left(\frac{3}{4} + 16\alpha^2 + \frac{747}{280} \varepsilon^2 \alpha^2\right) s^6 + O(s^7) \\
 &= \lim_{\delta \rightarrow 0} \frac{1}{\delta^2} - \frac{\sqrt{\pi} \Gamma\left(\frac{2}{3}\right)}{\Gamma\left(\frac{1}{6}\right)} \frac{1}{s^2} + \frac{\sqrt{\pi} \Gamma\left(\frac{1}{3}\right)}{6 \Gamma\left(\frac{5}{6}\right)} \left(1 + \frac{32}{3} \alpha^2 + \frac{281}{1260} \varepsilon^2 \alpha^2\right) s^2 \\
 &\quad - \frac{\sqrt{\pi} \Gamma\left(\frac{2}{3}\right)}{\Gamma\left(\frac{1}{6}\right)} \left(\frac{32}{3} \alpha^2 + \frac{467}{420} \varepsilon^2 \alpha^2\right) s^4 + \left(\frac{1}{4} + \frac{16}{3} \alpha^2 + \frac{249}{280} \varepsilon^2 \alpha^2\right) s^6 + O(s^7)
 \end{aligned}$$

Finally, we get $A_2(d)$ by using the relations (A.10) and (A.11), which is

$$\frac{A_2}{L_3 L_1} = \lim_{\delta \rightarrow 0} \frac{1}{\delta^2} + C_{31}^{-2} \frac{1}{d^2} + C_{31}^2 d^2 + C_{31}^4 d^4 + C_{31}^6 d^6 + O(d^7) \quad (\text{A.12})$$

where

$$\begin{aligned} C_{31}^{-2} &= -\frac{32\sqrt{\pi^9}}{3\sqrt{3}} \frac{1}{\Gamma\left(\frac{1}{3}\right)^3 \Gamma\left(\frac{1}{6}\right)^3} \\ C_{31}^2 &= \frac{3}{320\sqrt{\pi^7}} \Gamma\left(\frac{1}{3}\right)^3 \Gamma\left(\frac{1}{6}\right)^3 \left(1 + \frac{32}{3}\alpha^2 + \frac{281}{1260}\varepsilon^2\alpha^2\right) \\ C_{31}^4 &= -\frac{3\sqrt{3}}{28\sqrt{\pi^9}} \Gamma\left(\frac{1}{3}\right)^3 \Gamma\left(\frac{1}{6}\right)^3 \left(\alpha^2 + \frac{467}{4480}\varepsilon^2\alpha^2\right) \\ C_{31}^6 &= \frac{27}{16384\pi^9} \Gamma\left(\frac{1}{3}\right)^6 \Gamma\left(\frac{1}{6}\right)^6 \left(1 - \frac{13\sqrt{3}}{1800\pi^{5/2}} \Gamma\left(\frac{1}{3}\right)^3 \Gamma\left(\frac{1}{6}\right)^3\right) \\ &\quad + \frac{9}{256\pi^9} \Gamma\left(\frac{1}{3}\right)^6 \Gamma\left(\frac{1}{6}\right)^6 \left(1 - \frac{13\sqrt{3}}{1800\pi^{5/2}} \Gamma\left(\frac{1}{3}\right)^3 \Gamma\left(\frac{1}{6}\right)^3\right) \alpha^2 \\ &\quad - \frac{6723}{1146880\pi^9} \Gamma\left(\frac{1}{3}\right)^6 \Gamma\left(\frac{1}{6}\right)^6 \left(1 + \frac{3653\sqrt{3}}{4033800\pi^{5/2}} \Gamma\left(\frac{1}{3}\right)^3 \Gamma\left(\frac{1}{6}\right)^3\right) \varepsilon^2 \alpha^2, \end{aligned}$$

B Equations and solutions for the long cylinder

B.1 Solutions for $z_0(\rho)$, $z^{(\alpha)}(\rho)$ and $z^{(\varepsilon)}(\rho)$

As we discussed in section 4, we solve equation (4.3) by employing small α and ε expansion upto leading order in α^2 and $\varepsilon^2\alpha^2$. The form of the solution is given by

$$z(\rho) = z_0(\rho) + \alpha^2 z^{(\alpha)}(\rho) + \varepsilon^2 \alpha^2 z^{(\varepsilon)}(\rho), \quad (\text{B.1})$$

and each $z_0, z^{(\alpha)}, z^{(\varepsilon)}$ can be solved in the form of series solution in ρ . With such a form of the solution (B.1), we consider small α^2 and ε^2 expansion of equation (4.3) and solve equations of zeroth order in α and ε , of leading order in α^2 , and $\varepsilon^2\alpha^2$.

First, let us examine the equation for z_0 , which is zeroth order in α and ε , being given by

$$\sqrt{1 + \frac{(z_0')^2}{1 - z_0^4}} - z_0^3 \frac{\partial}{\partial \rho} \left(\frac{\rho}{z_0^3 \sqrt{1 + \frac{(z_0')^2}{1 - z_0^4}}} \right) = 0, \quad (\text{B.2})$$

where prime denotes derivative with respect to ρ . The solution for z_0 is given by

$$\begin{aligned} z_0 &= z_* + \frac{3(z_*^4 - 1)}{4z_*} \rho^2 + \frac{9(7z_*^8 - 2z_*^4 - 5)}{128z_*^3} \rho^4 + \frac{3(10z_*^{12} - 13z_*^8 + 16z_*^4 - 13)}{128z_*^5} \rho^6 \\ &\quad + \frac{9(1275z_*^{16} - 2456z_*^{12} - 1354z_*^8 + 7216z_*^4 - 4681)}{131072z_*^7} \rho^8 \\ &\quad + \frac{27(23275z_*^{20} - 49367z_*^{16} + 36878z_*^{12} - 184910z_*^8 + 356407z_*^4 - 182283)}{13107200z_*^9} \rho^{10} \dots \\ &\quad + \text{upto } O(\rho^{38}), \end{aligned} \quad (\text{B.3})$$

where we get the series solution upto order of ρ^{38} but we just write the solution upto $O(\rho^{10})$. To get the relation between a and z_* , we apply the boundary condition (4.7). The relation is obtained numerically. Some results are given in table 1. In fact, to draw the graphs, we obtain more data points.

The equation of $z^{(\alpha)}(\rho)$ is given by

$$\begin{aligned} & \frac{1}{2} \frac{z_0'}{z_0^3} \frac{z_0' N_\alpha + 2z^{(\alpha)'} + \frac{4z^{(\alpha)} z_0'^3 z_0'}{1-z_0^4}}{1-z_0^4 + (z_0')^2} \sqrt{1 + \frac{(z_0')^2}{1-z_0^4}} - 3 \frac{z^{(\alpha)}}{z_0^4} \sqrt{1 + \frac{(z_0')^2}{1-z_0^4}} \\ &= \frac{\partial}{\partial \rho} \left[-\frac{1}{2} \rho \frac{z_0'}{z_0^3} \frac{z_0' N_\alpha + 2z^{(\alpha)'} + \frac{4z^{(\alpha)} z_0'^3 z_0'}{1-z_0^4}}{1-z_0^4 + (z_0')^2} \frac{1}{\sqrt{1 + \frac{(z_0')^2}{1-z_0^4}}} - 3\rho \frac{z^{(\alpha)}}{z_0^4} \frac{1}{\sqrt{1 + \frac{(z_0')^2}{1-z_0^4}}} \right], \end{aligned} \quad (\text{B.4})$$

where

$$N_\alpha = \frac{32}{3} \frac{z_0^4}{1+z_0^2}. \quad (\text{B.5})$$

We note that the equation is that of leading order in α^2 . We put the zeroth order solution, z_0 that we obtained previously into the equation (B.4) and get the solution of $z^{(\alpha)}(\rho)$ which is also a series solution in small ρ . The solution, $z^{(\alpha)}(\rho)$ is given by

$$\begin{aligned} z^{(\alpha)} &= z_*^\alpha + \frac{9z_*^4 z_*^\alpha + 3z_*^\alpha - 32z_*^7 + 32z_*^5}{4z_*^2} \rho^2 \\ &+ \frac{315z_*^8 z_*^\alpha - 18z_*^4 z_*^\alpha + 135z_*^\alpha - 1920z_*^{11} + 1344z_*^9 + 768z_*^7 - 192z_*^5}{128z_*^4} \rho^4 \\ &+ \frac{1}{128z_*^6} \left(210z_*^{12} z_*^\alpha - 117z_*^8 z_*^\alpha - 48z_*^4 z_*^\alpha + 195z_*^\alpha \right. \\ &\left. - 2000z_*^{15} + 960z_*^{13} + 2272z_*^{11} - 832z_*^9 - 912z_*^7 + 512z_*^5 \right) \rho^6 \dots + \text{upto } O(\rho^{30}) \end{aligned} \quad (\text{B.6})$$

We also get the equation and the solution for $z^{(\epsilon)}$, being given by

$$\begin{aligned} & \frac{1}{2} \frac{z_0'}{z_0^3} \frac{z_0' (N_\epsilon + 2F) + 2z^{(\epsilon)'} + \frac{4z^{(\epsilon)} z_0'^3 z_0'}{1-z_0^4}}{1-z_0^4 + (z_0')^2} \sqrt{1 + \frac{(z_0')^2}{1-z_0^4}} - 3 \frac{z^{(\epsilon)}}{z_0^4} \sqrt{1 + \frac{(z_0')^2}{1-z_0^4}} \\ &= \frac{\partial}{\partial \rho} \left[-\frac{1}{2} \rho \frac{z_0'}{z_0^3} \frac{z_0' (N_\epsilon + 2F) + 2z^{(\epsilon)'} + \frac{4z^{(\epsilon)} z_0'^3 z_0'}{1-z_0^4}}{1-z_0^4 + (z_0')^2} \frac{1}{\sqrt{1 + \frac{(z_0')^2}{1-z_0^4}}} - 3\rho \frac{z^{(\epsilon)}}{z_0^4} \frac{1}{\sqrt{1 + \frac{(z_0')^2}{1-z_0^4}}} \right], \end{aligned} \quad (\text{B.7})$$

where

$$N_\epsilon = \frac{4}{9} z_0^4 \left(\frac{281}{560} - \frac{2z_0^6 + 6z_0^4 + 3z_0^2}{2(z_0^2 + 1)^4} \right), \quad (\text{B.8})$$

$$F = \frac{1}{18} z_0^6 \frac{z_0^2 - 2}{(z_0^2 + 1)^4}. \quad (\text{B.9})$$

The solution of $z^{(\varepsilon)}$ is given by

$$\begin{aligned}
 z^{(\varepsilon)} = & z_*^\varepsilon + \frac{1}{1680z_*^2(z_*^2+1)^3} \left(3780z_*^{10}z_*^\varepsilon + 11340z_*^8z_*^\varepsilon + 12600z_*^6z_*^\varepsilon + 7560z_*^4z_*^\varepsilon + 3780z_*^2z_*^\varepsilon \right. \\
 & \left. + 1260z_*^\varepsilon - 281z_*^{15} - 283z_*^{13} + 418z_*^{11} + 142z_*^9 - 277z_*^7 + 281z_*^5 \right) \rho^2 \\
 & + \frac{1}{8960z_*^4(z_*^2+1)^3} \left(22050z_*^{14}z_*^\varepsilon + 66150z_*^{12}z_*^\varepsilon + 64890z_*^{10}z_*^\varepsilon + 18270z_*^8z_*^\varepsilon + 5670z_*^6z_*^\varepsilon \right. \\
 & \left. + 27090z_*^4z_*^\varepsilon + 28350z_*^2z_*^\varepsilon + 9450z_*^\varepsilon - 3653z_*^{19} - 5359z_*^{17} + 4875z_*^{15} + 8009z_*^{13} - 3179z_*^{11} \right. \\
 & \left. - 4049z_*^9 + 3637z_*^7 - 281z_*^5 \right) \rho^4 \\
 & + \frac{1}{53760z_*^6(z_*^2+1)^3} \left(88200z_*^{18}z_*^\varepsilon + 264600z_*^{16}z_*^\varepsilon + 215460z_*^{14}z_*^\varepsilon - 59220z_*^{12}z_*^\varepsilon - 167580z_*^{10}z_*^\varepsilon \right. \\
 & \left. - 109620z_*^8z_*^\varepsilon + 21420z_*^6z_*^\varepsilon + 225540z_*^4z_*^\varepsilon + 245700z_*^2z_*^\varepsilon + 81900z_*^\varepsilon - 31191z_*^{23} - 58573z_*^{21} \right. \\
 & \left. + 40445z_*^{19} + 121103z_*^{17} + 31111z_*^{15} - 89251z_*^{13} - 33693z_*^{11} + 61985z_*^9 - 18432z_*^7 + 4496z_*^5 \right) \rho^6 \\
 & + \text{upto } O(\rho^{30})
 \end{aligned}
 \tag{B.10}$$

B.2 Black brane solution and entanglement temperature

In this subsection, we find the solutions of z_0^A and z_0^B . In this case, $f(r)$ and $N(r)$ are given by

$$f = 1, \quad N(r, \xi) = r^2 - \frac{\xi}{r^2},$$

and z_0 will have a form of

$$z_0 = z_0^A + \xi z_0^B + O(\xi^2),$$

where ξ is a bookkeeping parameter and later we take $\xi = 1$. The equation of z_0 is given by

$$\sqrt{1 + \frac{(z_0')^2}{1 - \xi z_0^4}} - z_0^3 \frac{\partial}{\partial \rho} \left(\frac{\rho}{z_0^3 \sqrt{1 + \frac{(z_0')^2}{1 - \xi z_0^4}}} \right) = 0. \tag{B.11}$$

The solutions for z_0^A and z_0^B are obtained by employing power expansion order by order in ξ upto its first order. We get series solutions for z_0^A and z_0^B in ρ upto $O(\rho^{75})$, which are given by

$$\begin{aligned}
 z_0^A = & z_*^A - \frac{3}{4(z_*^A)^2} \rho^2 - \frac{45}{128(z_*^A)^3} \rho^4 - \frac{39}{128(z_*^A)^5} \rho^6 + \dots, \\
 z_0^B = & z_*^B + \frac{3(z_*^A)^5 + 3z_*^B}{4(z_*^A)^2} \rho^2 + \frac{-18(z_*^A)^5 + 135z_*^B}{128(z_*^A)^4} \rho^4 + \frac{48(z_*^A)^5 + 195z_*^B}{128(z_*^A)^6} \rho^6 + \dots.
 \end{aligned}
 \tag{B.12}$$

The boundary condition $z_0^A(a) = 0$ gives a constant ratio of a to z_*^A as

$$\frac{a}{z_*^A} = 0.789541. \tag{B.13}$$

With the given values of a from the previous computation, the boundary condition $z_0^B(a) = 0$ gives the value of z_*^B . With these values we obtain

$$\lim_{a \rightarrow 0} \frac{\gamma^{(\xi)}}{a^3} = 0.73228506. \quad (\text{B.14})$$

The solution of $\gamma^{(\xi)}(a)$ is given explicitly in the next subsection, upto 6th order.

B.3 Computation of the surface area for cylinder

Defining $r \equiv z^{-1}(\rho)$, the integral for the surface area of the cylinder becomes

$$A_1^{cy} = 2\pi L_1 \int_a^0 z^{-3}(\rho) \rho \left(\frac{\partial z}{\partial \rho} \right) d\rho \sqrt{\frac{1}{\left(\frac{\partial z}{\partial \rho} \right)^2} + \frac{1}{z^2 N(z^{-1}) f^2(z^{-1})}}. \quad (\text{B.15})$$

We expand the integrand upto leading order of ξ , α^2 , and $\varepsilon^2 \alpha^2$, as we similarly did for $z(\rho)$:

$$A_1^{cy} = 2\pi L_1 \left(\gamma^{(AdS)} + \xi \gamma^{(\xi)} + \alpha^2 \gamma^{(\alpha)} + \varepsilon^2 \alpha^2 \gamma^{(\varepsilon)} \right).$$

The solutions of $z^{(\alpha)}(\rho)$, $z^{(\varepsilon)}(\rho)$, $z_0^A(\rho)$ and $z_0^B(\rho)$ are given in appendix B.1 and B.2. With these solutions we may expand the integrands in terms of ρ and integrate them to get $\gamma^{(\xi)}$, $\gamma^{(\alpha)}$, and $\gamma^{(\varepsilon)}$:

$$\gamma^{(\xi)} = -\frac{3z_*^B}{2(z_*^A)^4} a^2 - \frac{27\{(z_*^A)^5 + 5z_*^B\}}{32(z_*^A)^6} a^4 - \frac{45\{3(z_*^A)^5 + 14z_*^B\}}{64(z_*^A)^8} a^6 + \text{upto } O(a^{75}), \quad (\text{B.16})$$

$$\begin{aligned} \gamma^{(\alpha)} = & -\frac{3z_*^{(\alpha)}}{2z_*^4} a^2 + \frac{9(-32z_*^5 + 32z_*^7 - 15z_*^{(\alpha)} + 3z_*^4 z_*^{(\alpha)})}{32z_*^6} a^4 \\ & - \frac{15(96z_*^5 - 80z_*^7 - 64z_*^9 + 48z_*^{11} + 42z_*^{(\alpha)} - 27z_*^4 z_*^{(\alpha)} - 3z_*^8 z_*^{(\alpha)})}{64z_*^8} a^6 + \text{upto } O(a^{30}), \end{aligned} \quad (\text{B.17})$$

$$\begin{aligned} \gamma^{(\varepsilon)} = & -\frac{3z_*^{(\varepsilon)}}{2z_*^4} a^2 \\ & + \frac{3}{4480z_*^6(z_*^2 + 1)^3} \left\{ -281z_*^5 + 277z_*^7 - 142z_*^9 - 418z_*^{11} + 283z_*^{13} + 281z_*^{15} \right. \\ & + z_*^{(\varepsilon)} \left. (-6300 - 18900z_*^2 - 17640z_*^4 - 2520z_*^6 + 3780z_*^8 + 1260z_*^{10}) \right\} a^4 \\ & + \frac{1}{1792z_*^8(1 + z_*^2)^3} \left\{ -843z_*^5 + 271z_*^7 + 1115z_*^9 - 1671z_*^{11} + 11z_*^{13} + 1401z_*^{15} - 3z_*^{17} \right. \\ & - 281z_*^{19} + z_*^{(\varepsilon)} \left. (-17640 + 52920z_*^2 - 41580z_*^4 + 16380z_*^6 + 35280z_*^8 + 15120z_*^{10} \right. \\ & \left. + 3780z_*^{12} + 1260z_*^{14}) \right\} a^6 + \text{upto } O(a^{30}). \end{aligned} \quad (\text{B.18})$$

Open Access. This article is distributed under the terms of the Creative Commons Attribution License ([CC-BY 4.0](https://creativecommons.org/licenses/by/4.0/)), which permits any use, distribution and reproduction in any medium, provided the original author(s) and source are credited. SCOAP³ supports the goals of the International Year of Basic Sciences for Sustainable Development.

References

- [1] O. Aharony, S.S. Gubser, J.M. Maldacena, H. Ooguri and Y. Oz, *Large N field theories, string theory and gravity*, *Phys. Rept.* **323** (2000) 183 [[hep-th/9905111](#)] [[INSPIRE](#)].
- [2] J.M. Maldacena, *The Large N limit of superconformal field theories and supergravity*, *Adv. Theor. Math. Phys.* **2** (1998) 231 [[hep-th/9711200](#)] [[INSPIRE](#)].
- [3] J.-H. Oh, *Gauge-gravity Duality and its Applications to Cosmology and Fluid Dynamics*, Ph.D. thesis, Kentucky University (2011) [[INSPIRE](#)].
- [4] P. Kovtun, D.T. Son and A.O. Starinets, *Viscosity in strongly interacting quantum field theories from black hole physics*, *Phys. Rev. Lett.* **94** (2005) 111601 [[hep-th/0405231](#)] [[INSPIRE](#)].
- [5] P. Benincasa, A. Buchel and R. Naryshkin, *The Shear viscosity of gauge theory plasma with chemical potentials*, *Phys. Lett. B* **645** (2007) 309 [[hep-th/0610145](#)] [[INSPIRE](#)].
- [6] N. Iqbal and H. Liu, *Universality of the hydrodynamic limit in AdS/CFT and the membrane paradigm*, *Phys. Rev. D* **79** (2009) 025023 [[arXiv:0809.3808](#)] [[INSPIRE](#)].
- [7] S.A. Hartnoll, *Lectures on holographic methods for condensed matter physics*, *Class. Quant. Grav.* **26** (2009) 224002 [[arXiv:0903.3246](#)] [[INSPIRE](#)].
- [8] C.P. Herzog, *Lectures on Holographic Superfluidity and Superconductivity*, *J. Phys. A* **42** (2009) 343001 [[arXiv:0904.1975](#)] [[INSPIRE](#)].
- [9] G.T. Horowitz, *Introduction to Holographic Superconductors*, *Lect. Notes Phys.* **828** (2011) 313 [[arXiv:1002.1722](#)] [[INSPIRE](#)].
- [10] S.S. Gubser, *Breaking an Abelian gauge symmetry near a black hole horizon*, *Phys. Rev. D* **78** (2008) 065034 [[arXiv:0801.2977](#)] [[INSPIRE](#)].
- [11] S.S. Gubser, *Colorful horizons with charge in anti-de Sitter space*, *Phys. Rev. Lett.* **101** (2008) 191601 [[arXiv:0803.3483](#)] [[INSPIRE](#)].
- [12] S.A. Hartnoll, C.P. Herzog and G.T. Horowitz, *Holographic Superconductors*, *JHEP* **12** (2008) 015 [[arXiv:0810.1563](#)] [[INSPIRE](#)].
- [13] C.P. Herzog and S.S. Pufu, *The Second Sound of $SU(2)$* , *JHEP* **04** (2009) 126 [[arXiv:0902.0409](#)] [[INSPIRE](#)].
- [14] P. Basu, J. He, A. Mukherjee and H.-H. Shieh, *Superconductivity from $D3/D7$: Holographic Pion Superfluid*, *JHEP* **11** (2009) 070 [[arXiv:0810.3970](#)] [[INSPIRE](#)].
- [15] S. Ryu and T. Takayanagi, *Holographic derivation of entanglement entropy from AdS/CFT*, *Phys. Rev. Lett.* **96** (2006) 181602 [[hep-th/0603001](#)] [[INSPIRE](#)].
- [16] S. Ryu and T. Takayanagi, *Aspects of Holographic Entanglement Entropy*, *JHEP* **08** (2006) 045 [[hep-th/0605073](#)] [[INSPIRE](#)].
- [17] J. Erdmenger, P. Kerner and H. Zeller, *Non-universal shear viscosity from Einstein gravity*, *Phys. Lett. B* **699** (2011) 301 [[arXiv:1011.5912](#)] [[INSPIRE](#)].
- [18] P. Basu and J.-H. Oh, *Analytic Approaches to Anisotropic Holographic Superfluids*, *JHEP* **07** (2012) 106 [[arXiv:1109.4592](#)] [[INSPIRE](#)].
- [19] J.-H. Oh, *Running Shear Viscosities in An-Isotropic Holographic Superfluids*, *JHEP* **06** (2012) 103 [[arXiv:1201.5605](#)] [[INSPIRE](#)].

- [20] M. Park, J. Park and J.-H. Oh, *Phase transition in anisotropic holographic superfluids with arbitrary dynamical critical exponent z and hyperscaling violation factor α* , *Eur. Phys. J. C* **77** (2017) 810 [[arXiv:1609.08241](#)] [[INSPIRE](#)].
- [21] S.N. Solodukhin, *Entanglement entropy, conformal invariance and extrinsic geometry*, *Phys. Lett. B* **665** (2008) 305 [[arXiv:0802.3117](#)] [[INSPIRE](#)].
- [22] L.-Y. Hung, R.C. Myers and M. Smolkin, *On Holographic Entanglement Entropy and Higher Curvature Gravity*, *JHEP* **04** (2011) 025 [[arXiv:1101.5813](#)] [[INSPIRE](#)].
- [23] H. Casini, M. Huerta and R.C. Myers, *Towards a derivation of holographic entanglement entropy*, *JHEP* **05** (2011) 036 [[arXiv:1102.0440](#)] [[INSPIRE](#)].
- [24] J. Bhattacharya, M. Nozaki, T. Takayanagi and T. Ugajin, *Thermodynamical Property of Entanglement Entropy for Excited States*, *Phys. Rev. Lett.* **110** (2013) 091602 [[arXiv:1212.1164](#)] [[INSPIRE](#)].
- [25] E. Bianchi and R.C. Myers, *On the Architecture of Spacetime Geometry*, *Class. Quant. Grav.* **31** (2014) 214002 [[arXiv:1212.5183](#)] [[INSPIRE](#)].
- [26] M. Nozaki, T. Numasawa, A. Prudenziati and T. Takayanagi, *Dynamics of Entanglement Entropy from Einstein Equation*, *Phys. Rev. D* **88** (2013) 026012 [[arXiv:1304.7100](#)] [[INSPIRE](#)].
- [27] D. Allahbakhshi, M. Alishahiha and A. Naseh, *Entanglement Thermodynamics*, *JHEP* **08** (2013) 102 [[arXiv:1305.2728](#)] [[INSPIRE](#)].
- [28] G. Wong, I. Klich, L.A. Pando Zayas and D. Vaman, *Entanglement Temperature and Entanglement Entropy of Excited States*, *JHEP* **12** (2013) 020 [[arXiv:1305.3291](#)] [[INSPIRE](#)].
- [29] D. Momeni, M. Raza, H. Gholizade and R. Myrzakulov, *Realization of Holographic Entanglement Temperature for a Nearly-AdS boundary*, *Int. J. Theor. Phys.* **55** (2016) 4751 [[arXiv:1505.00215](#)] [[INSPIRE](#)].
- [30] C. Park, *Holographic Aspects of a Relativistic Nonconformal Theory*, *Adv. High Energy Phys.* **2013** (2013) 389541 [[arXiv:1209.0842](#)] [[INSPIRE](#)].
- [31] C. Park, *Thermodynamic law from the entanglement entropy bound*, *Phys. Rev. D* **93** (2016) 086003 [[arXiv:1511.02288](#)] [[INSPIRE](#)].
- [32] K.-S. Kim and C. Park, *Renormalization group flow of entanglement entropy to thermal entropy*, *Phys. Rev. D* **95** (2017) 106007 [[arXiv:1610.07266](#)] [[INSPIRE](#)].
- [33] H.-S. Jeong, K.-Y. Kim and Y.-W. Sun, *Holographic entanglement density for spontaneous symmetry breaking*, *JHEP* **06** (2022) 078 [[arXiv:2203.07612](#)] [[INSPIRE](#)].
- [34] L.-Y. Hung, R.C. Myers, M. Smolkin and A. Yale, *Holographic Calculations of Renyi Entropy*, *JHEP* **12** (2011) 047 [[arXiv:1110.1084](#)] [[INSPIRE](#)].
- [35] M. Huerta, *Numerical Determination of the Entanglement Entropy for Free Fields in the Cylinder*, *Phys. Lett. B* **710** (2012) 691 [[arXiv:1112.1277](#)] [[INSPIRE](#)].
- [36] S. Banerjee, Y. Nakaguchi and T. Nishioka, *Renormalized Entanglement Entropy on Cylinder*, *JHEP* **03** (2016) 048 [[arXiv:1508.00979](#)] [[INSPIRE](#)].
- [37] M.P. Hertzberg and F. Wilczek, *Some Calculable Contributions to Entanglement Entropy*, *Phys. Rev. Lett.* **106** (2011) 050404 [[arXiv:1007.0993](#)] [[INSPIRE](#)].
- [38] A. Lewkowycz, R.C. Myers and M. Smolkin, *Observations on entanglement entropy in massive QFT's*, *JHEP* **04** (2013) 017 [[arXiv:1210.6858](#)] [[INSPIRE](#)].

- [39] V. Rosenhaus and M. Smolkin, *Entanglement Entropy: A Perturbative Calculation*, *JHEP* **12** (2014) 179 [[arXiv:1403.3733](#)] [[INSPIRE](#)].
- [40] V. Rosenhaus and M. Smolkin, *Entanglement Entropy for Relevant and Geometric Perturbations*, *JHEP* **02** (2015) 015 [[arXiv:1410.6530](#)] [[INSPIRE](#)].
- [41] C. Park, *Logarithmic Corrections to the Entanglement Entropy*, *Phys. Rev. D* **92** (2015) 126013 [[arXiv:1505.03951](#)] [[INSPIRE](#)].
- [42] R.E. Arias and I.S. Landea, *Backreacting p-wave Superconductors*, *JHEP* **01** (2013) 157 [[arXiv:1210.6823](#)] [[INSPIRE](#)].
- [43] R.-G. Cai, S. He, L. Li and Y.-L. Zhang, *Holographic Entanglement Entropy on P-wave Superconductor Phase Transition*, *JHEP* **07** (2012) 027 [[arXiv:1204.5962](#)] [[INSPIRE](#)].